Engineered Barrier System R&D and International Collaborations – LANL (FY18)

Fuel Cycle Technology

Prepared for
U.S. Department of Energy
Spent Fuel & Waste Science and Tech
Caporuscio, F.A.
Sauer, K.B.
Rock, M. J.
Houser, L. M.
Los Alamos National Laboratory

August 10, 2018
SF-18LA01030801/SF-18LA01030805
'LA-UR-18- 27601'

DISCLAIMER

This information was prepared as an account of work sponsored by an agency of the U.S. Government. Neither the U.S. Government nor any agency thereof, nor any of their employees, makes any warranty, expressed or implied, or assumes any legal liability or responsibility for the accuracy, completeness, or usefulness, of any information, apparatus, product, or process disclosed, or represents that its use would not infringe privately owned rights. References herein to any specific commercial product, process, or service by trade name, trade mark, manufacturer, or otherwise, does not necessarily constitute or imply its endorsement, recommendation, or favoring by the U.S. Government or any agency thereof. The views and opinions of authors expressed herein do not necessarily state or reflect those of the U.S. Government or any agency thereof.

SUMMARY

The International Engineered Barrier System (IEBS) project has a focus on natural barrier systems and engineered barrier system aspects related to the EBS work package of the Spent Fuel and Waste Science and Technology R&D (SFWST). The U.S. Department of Energy is investigating the design and safety function of generic nuclear geologic repositories in a variety of geologic settings. The evaluation of the International Engineered Barrier System (IEBS) concepts and interaction with the wall rock (i.e., natural barriers), waste canisters, or other IEBS interfaces are important to the long-term performance and safety of geologic repositories (Nutt et al., 2011; Jove-Colon et al., 2011). The European community, especially the French, have investigated bentonite stability in contact with steel under a variety of experimental conditions in an attempt to replicate repository conditions (Pusch, 1979; Madsen, 1998; Meunier et al., 1998; Guillaume et al., 2003; Wersin et al., 2007; Mosser-Ruck et al., 2010; Ferrage et al., 2011, Mosser-Ruck et al., 2016). The majority of their research was focused on lower temperature environments and atmospheric pressures. They have never incorporated crystalline wall rock as part of their experiments.

Our experimental program for FY18 aims to 1) characterize how IEBS components (steel, Grimsel Granodiorite wall rock) react and change in the presence of Wyoming bentonite and 2) capture steel corrosion rates and interface mineralogy at reasonably high temperature (up to 250°C, 150 bar) in-situ repository conditions. Since this is a new line of research for SFWST, and experiments are of long duration (~6 weeks), we will report on two experiments for this report. The objective of this IEBS study is to determine the Grimsel Granodiorite host rock/groundwater interactions with bentonite and the steel canister at elevated pressure/ temperature (250oC, 150 bar) conditions. The baseline experiment (IEBS-1) consists of bentonite, Grimsel granodiorite, and synthetic groundwater to match the Grimsel site. The second experiment (IEBS-2) added coupons of 316 stainless steel to the mix of bentonite, Grimsel granodiorite, and synthetic groundwater to match the Grimsel site. Further experiments are ongoing at this time.

Outreach to other international programs based at Mont Terri, Grimsel, Stripa, and perhaps Japan and South Korea will be coordinated with the DOE international program lead (Jens Birkholzer). The intent is to share our experimental results in both Argillite and Crystalline rock EBS platforms with international government entities. This will entail correspondence, travel to their research sites (URLs), international workshops, conferences, and cooperative research.

CONTENTS

FIGURES

TABLES

ACRONYMS

EBS – Engineered Barrier Systems

EDX – Energy Dispersive X-ray

EMP - Electron Microprobe

FY – Fiscal Year

IAEA – International Atomic Energy Association

IC - Ion Chromatography

IEBS – International Engineered Barrier System

MPa – Mega Pascal

QXRD- Quantitative X-ray Diffraction

SEM - Scanning Electron Microscope

SFWST - Spent Fuel and Waste Science and Technology R&D

SS – Stainless Steel

XRD - X-ray Diffraction

ENGINEERED BARRIER SYSTEM R&D AND INTERNATIONAL COLLABORATIONS – LANL

1. INTRODUCTION

The U.S. Department of Energy's Spent Fuel and Waste Science and Technology R&D (SFWST) Campaign is investigating the design and safety function of generic nuclear geologic repositories in a variety of geologic settings. The evaluation of the International Engineered Barrier System (IEBS) concepts and interaction with the wall rock (i.e., natural barriers), waste canisters, or other IEBS interfaces are important to the long-term performance and safety of geologic repositories (Nutt et al., 2011; Jove-Colon et al., 2011). The European community, especially the French, have investigated bentonite stability in contact with steel under a variety of experimental conditions in an attempt to replicate repository conditions (Pusch, 1979; Madsen, 1998; Meunier et al., 1998; Guillaume et al., 2003; Wersin et al., 2007; Mosser-Ruck et al., 2010; Ferrage et al., 2011, Mosser-Ruck et al., 2016). The majority of their research was focused on lower temperature environments and atmospheric pressures. Our experimental program for FY18 aims to 1) characterize how IEBS components (steel, Grimsel Granodiorite wall rock) react and change in the presence of Wyoming bentonite and 2) capture steel corrosion rates and interface mineralogy at reasonable high temperature (up to 250 °C, 150 bar) in-situ repository conditions.

1.1 Background and Objective

This IEBS collaboration has a focus on natural barrier systems and engineered barrier system aspects related to the EBS work package of the Spent Fuel and Waste Science and Technology R&D (SFWST). There are multiple international analytical programs with planned experimental setup to enable studying a number of issues relevant for repository design. The objective of this IEBS study was to determine the Grimsel Granodiorite host rock/groundwater interactions with bentonite and the steel canister at elevated pressure/temperature (250 °C, 150 bar) conditions (see Table 1). The groundwater composition at the Grimsel site is well characterized (Table 2). There is an ancillary work (Argillite R&D) that characterized Full Scale High-Level Waste Engineered Barrier System Experiment-Dismantling Project (FEBEX-DP)

materials which served as a lower P,T analog to the experiments presented here. A description of the FEBEX experiment is described in the next section.

The Grimsel Test Site (GTS) is located in the Swiss Alps near the Grimsel Pass (Bern Canton, Switzerland). The site was established in 1984 as a center for underground Research and Development (R&D) supporting the geological disposal of radioactive waste (Grimsel, 2017). The FEBEX is a 1:1 scale demonstration project for the emplacement of Spent Nuclear Fuel (SNF). The FEBEX tunnel proper is located in Grimsel granodiorite at a depth of 450 meters below the surface. This is an in situ migration experiment conducted between boreholes situated in sparsely fractured crystalline, Grimsel granodiorite, host rock focusing on bentonite solubility, colloidal mineral migration/formation, and colloid-associated radionuclide transport. Two heaters replicating SNF canisters (4.5 meters long, 12 ton each) were emplaced and surrounded by blocks of compacted bentonite clay. In February 1997, heaters were switched on and data acquisition began. The experiment ran from February 1997 to 2002 at a constant temperature of 180 °C at the surface of the canister (FEBEX, 2014). After the heating of the first canister was stopped and that portion (including the canister) of the experiment was excavated. After removal, a dummy canister (no heating capability) was emplaced, EBS blocks were reinserted, and a concrete plug was constructed. The second portion of the experiment ran until 2015, when full excavation of FEBEX was initiated.

Table 1: Initial components and reaction conditions for the IEBS experiments.

Experiment	Clay (g)	Brine (g)	IEBS Components	Run Temp (°C)	Run Time
IEBS-1	10.91	144.0	Bentonite, and G.G. only	250	6 weeks
IEBS-2	11.02	182.0	Bentonite, G.G, 316 SS	250	6 weeks

G.G. = Grimsel Granodiorite

Table 2: Initial groundwater chemical composition from the experimental shear zone at the GTS used as the bases of the synthetic groundwater used in these experiments (Missana & Geckeis, 2006).

		[M]*	[M]**	[M]***
Cations	Na^+	$6.9x10^{-4}$	$7.0\text{-}7.2x10^{-4}$	$7.0x10^{-4}$
	K^+	$5.0x10^{-6}$	$1.8\text{-}4.6x10^{-6}$	$1.0\text{-}3.6x10^{-6}$
	Mg^{2+}	$6.2x10^{-7}$	$<1.0x10^{-5}$	$2.0\text{-}4.1x10^{-5}$
	Ca^{2+}	$1.4x10^{-4}$	$1.4\text{-}1.6x10^{-4}$	$1.4x10^{-4}$
	Sr^{2+}	$2.0x10^{-6}$	$2.4\text{-}2.6x10^{-6}$	$1.9\text{-}2.3x10^{-6}$
	Rb^+	$2.5x10^{-8}$	not determined	$1.6x10^{-8}$
	Cs^+	$5.0x10^{-9}$	$4.3x10^{-9}$	$3.8\text{-}7.5x10^{-9}$
	Li^+	not determined	$1.1x10^{-5}$	$1.2x10^{-5}$
Anions:	SO_4^{2-}	$6.1x10^{-5}$	$2.8\text{-}6.3x10^{-5}$	$1.8x10^{-4}$
	F^-	$6.1x10^{-5}$	$3.4x10^{-4}$	$3.2x10^{-4}$
	Cl^-	$1.6x10^{-4}$	$1.6\text{-}2.2x10^{-4}$	$1.4x10^{-4}$
	Br^-	$3.8x10^{-7}$	not determined	$3.6x10^{-7}$
	I^-	$1.0x10^{-9}$	$\leq 1.58x10^{-7}$	$7.9x10^{-10}$
	PO_4^{3-}	not determined	$<1.0x10^{-6}$	not determined
Other Species:	Si	$2.5x10^{-4}$	$3.4x10^{-4}$	$2.0x10^{-4}$
	CO_2	$<7.0x10^{-7}$	not determined	not determined
	O_2	$<3.0x10^{-8}$	not determined	not determined
	N_2	$7\text{-}8x10^{-4}$	not determined	not determined
	U	not determined	$<4.2x10^{-9}$	$1.3\text{-}6.3x10^{-10}$
	Th	not determined	$<2.1x10^{-9}$	$<2.2x10^{-10}$
	Ti	not determined	$1.5x10^{-8}$	$6.3x10^{-8}$
	Fe	not determined	$<5.4x10^{-7}$	$6.3x10^{-7}$
	Al	not determined	$3.0\text{-}4.0x10^{-6}$	$0.5\text{-}1.7x10^{-6}$
Calculated(3)	HCO_3^-	$2.9x10^{-4}$	$4.7x10^{-4}$	$1.4x10^{-4}$
	CO_3^- (CO_3^{2-})	$4.2x10^{-5}$	$<1.0x10^{-4}$	-
	OH^-	$1.3x10^{-5}$	not determined	not determined
	$H_3SiO_4^-$	$4.2x10^{-5}$	not determined	not determined
	H_4SiO_4	$2.1x10^{-4}$	not determined	not determined
pH		9.6±0.2	9.5±0.2	9.6
Ionic strength [M]		0.0012	not determined	
Temperature [°C]		12±1	not determined	
Electrical Conductivity [µS cm^{-1}]		103±5	93-103	12
Eh [mV]		<300	-200±50	106

* Data are compiled from Bajo et al. (1989), Aksoyoglu et al. (1990) and Eikenberg et al. (1991) and represent the top of the range of data reported in Tab. 3.3 of Frick et al. (1992).
** After Missana et. al. (2001)
*** Grimsel Colloid Exercise (NTB 90-01) PSI data from Degueldre et al. 1996a
M= molar

2. METHODS

Analytical methods (Experimental Setup, Mineral Characterization, and Aqueous Geochemical Analyses) remain unchanged from Caporuscio et al. (2014). They are listed in Appendix A for convenience.

Post-reaction steel coupons were mounted in epoxy then polished exposing the cross-sectioned surfaces. These mounts were then imaged using two different methods: SEM and reflected light microscopy. For each IEBS run 15 to 40 images will be taken for each method. These image locations will be mapped and chosen to give a random distribution of the corrosion in the coupons. All images will be analyzed in Photoshop where the thickness of the silicate interface reaction minerals (chlorite and Fe-saponite) and the depth of the corrosion will be measured and then labeled for future analysis. Corrosion rates will be determined by dividing the average corrosion depth by the number of days in the run.

2.1 XRD Sample Preparation

Samples were milled to a fine powder in a tungsten carbide ring mill. Approximately 0.2 g of 0.3 μm corundum (Buehler) was added to a 1 g aliquot of each sample. The corundum and sample mixtures were homogenized by dry milling in an alumina mortar and pestle. A thin layer of petroleum jelly was applied to a one-inch round glass slide. Homogenized mixtures of corundum and sample were loaded onto glass slides such to form a thin layer of sample across the entirety of the glass slide. Samples were then loaded into the X-ray diffractometer (XRD) for analysis.

2.2 XRD Instrument Type and Scan Conditions

All XRD measurements were made at the University of Texas at Austin using a Bruker D8 Advance. The instrument is equipped with a Cu source and a LynxEye detector. Instrument parameters and acquisition details are discussed in Appendix A.

2.3 Scan Processing: QXRD

Post-acquisition processing and quantitative XRD (QXRD) were performed using Bruker's DIFFRAC^{plus}Basic Evaluation Package (EVA v.15) and are detailed in Appendix A.

2.4 Aqueous Geochemical Analyses

Major cations and trace metals were analyzed via inductively coupled plasma-optical emission spectrometry (Perkin Elmer Optima 2100 DV) and inductively coupled plasma-mass spectrometry (Elan 6100) utilizing EPA methods 200.7 and 200.8. Methodology is described in Appendix A. Aqueous geochemical results are presented in Appendix B.

3. RESULTS

3.1 Starting Material Characteristics

Wyoming Bentonite: The bentonite used in this experimental work is mined from a reducing horizon in Colony, Wyoming. Unprocessed Wyoming bentonite contains primarily smectite with minor amounts of clinoptilolite and lesser plagioclase, biotite, calcite, and sulfide minerals. The QXRD results from unheated bentonite are presented in Table 3.

	Wyoming Bentonite	Grimsel Granodiorite
Analcime / Wairakite	b.d.l.	
Clinoptilolite	12.0	
Smectite	66.4	
Kaolinite	b.d.l.	
Albite		25.14
Plagioclase	8.3	
Orthoclase		30.84
Anorthite		
K-Feldspar	b.d.l.	
Biotite	2.8	
Muscovite		
Chlorite	b.d.l.	
Calcite	5.5	
Dolomite	+	
Quartz	0.9	44.02
Cristobalite/ Opal-C	1.8	
Pyrite	0.4	
Siderite	1.8	
Total:	100.0*	100.00

Table 3: Quantitative X-Ray Diffraction (QXRD) analyses of the buffer clay (Wyoming Bentonite) the wall rock (Opalinus Clay). Values are in weight percent. b.d.l. = below detection limit, * represents data set was normalized to 100.0, (+) represents material detectable but below 0.5 wt. %.

Grimsel Granodiorite: Major mineral phases are K-feldspar, plagioclase, and quartz. Minor phases are muscovite and biotite. Trace phases are allanite, zircon, titanite, and apatite. The QXRD results from unheated granodiorite are presented in Table 3 and Figure 1.

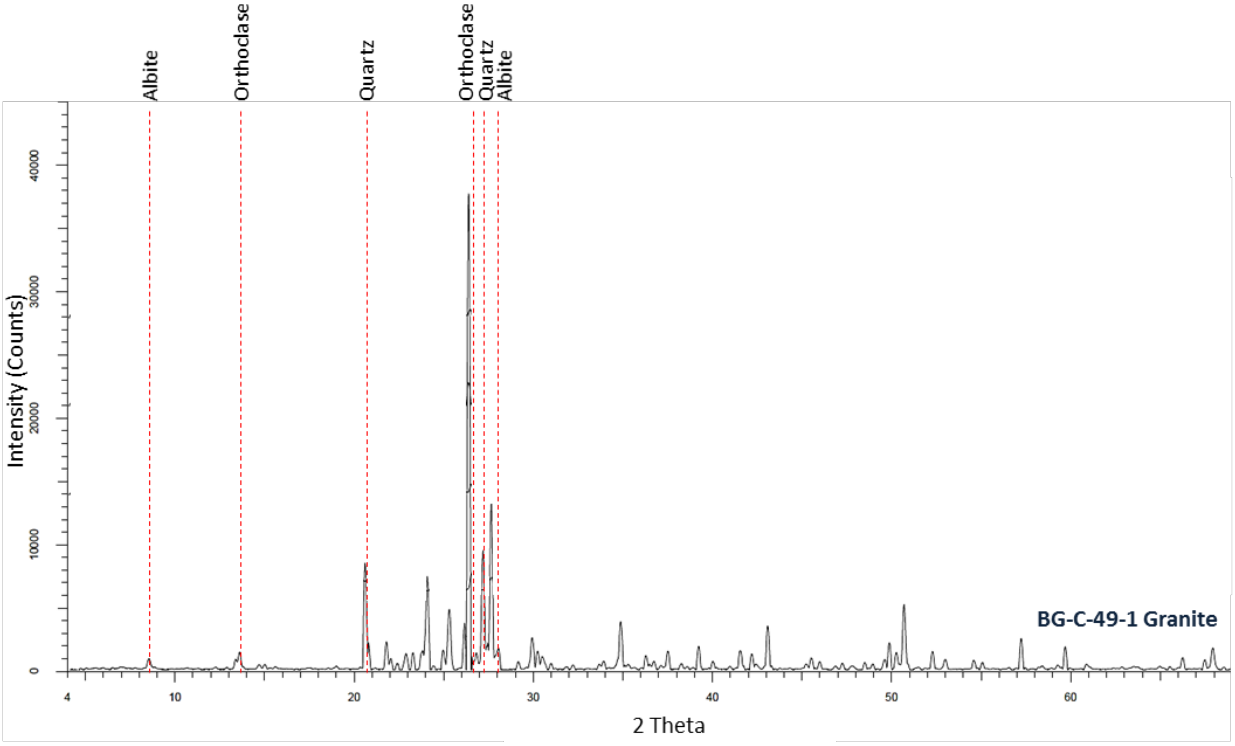

Figure 1. XRD pattern for the Grimsel granodiorite. The peaks are labeled to their corresponding minerals and unmarked peaks belong to the corundum standard.

Synthetic Grimsel groundwater: Synthetic groundwater (Table 4) was created to mimic the pore water found in the Grimsel Granodiorite (Missana & Geckeis, 2006). This solution has a pH of around 7.5 and the initial chemistry is reported in Table 4.

Table 4: Synthetic groundwater chemistry used in the IEBS experiments.

Components	Concentration (M)
Na_2SO4	$9.08x10^{-4}$
KCl	$6.44x10^{-5}$
$MgCO_3$	$5.06x10^{-4}$
$NaHCO_3$	$3.25x10^{-3}$
$CaCl_2$	$1.72x10^{-4}$
H_4SiO_4	$5.73x10^{-4}$

3.2 Results from IEBS-1 to IEBS-2

3.2.1 Aqueous Geochemistry

Water samples were collected periodically during the course of each experiment. The aqueous geochemistry results are reported and plotted in Appendix B, and described below.

pH

The starting solution for the IEBS experiments, Grimsel Granodiorite groundwater, has a pH of ~7.5. The pH of the fluid periodically extracted from the reaction vessels dropped over the course of both experiments. The pH of IEBS-1 initially dropped to ~7, and then remained ~6.5 for the experiment duration. Experiment IEBS-2 had a slightly more acidic solution during the middle of the experiment: the pH dropped to ~5 by week 3 and then increased to ~6.2 by the end of the experiment (Figure 5).

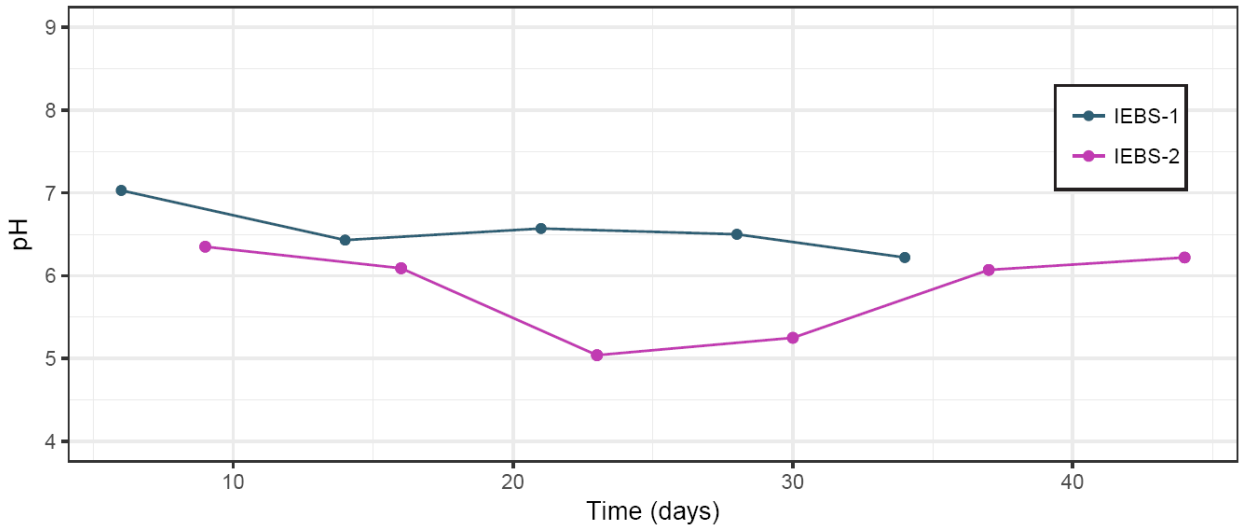

Figure 2. Solution pH from fluid collected throughout the duration of each IEBS experiment.

Cations

K^+, Na^+: In IEBS-1, the concentration of K^+ and Na^+ in solution decreases steadily during the experiment. The K^+ concentration for both filtered and unfiltered aliquots is initially ~2 mg/L and decreases to ~1.5 mg/L by week 6. The [Na^+] is ~150 mg/L at week 1 and reaches 120 mg/L by week 6.

In IEBS-2, the unfiltered K^+ concentration initially increases from ~1.7 mg/L in week 1 to ~2.2 mg/L in week 2 before dropping to between ~1.4–1.7 for the remainder of the experiment. The

[Na^+] decreases from ~140 mg/L to ~100 mg/L over the 6 week experiment. The filtered results show a large spike in [Na^+] and [K^+] around week two to 2000 mg/L and 100 mg/L, respectively. As this spike is not observed in the unfiltered results, it is likely not representative of chemical changes in the sample.

Ca^{2+}: In IEBS-1, the Ca^{2+} concentration in the filtered and unfiltered sample decreases steadily from ~2.0 to 1.0 mg/L over 6 weeks. The [Ca^{2+}] in the unfiltered sample in IEBS-2 is ~2.0 mg/L at the experiment start, drops to ~1.0 mg/L by week 3, and increases steadily to ~1.5 mg/L by the end of the run. The filtered sample shows a spike to ~90 mg/L around week 2.

SiO_2: The SiO_{2aq} concentration in IEBS-1 is higher in the filtered vs. unfiltered sample. Both stay between ~400 and 700 mg/L. The unfiltered results show an initial drop in concentration (weeks 1–3 followed by and increase to similar values as observed in the filtered sample by weeks 4 and 5 (~650–700 mg/L).

The filtered and unfiltered results from IEBS-2 show the same patterns for aqueous SiO_2. Concentrations remain around ~600 mg/L with the exception of a dip to ~500 and ~100 mg/L for unfiltered and filtered sample, respectively.

Fe^{2+}: The [Fe^{2+}] in both IEBS-1 and IEBS-2 remains relatively constant between ~0.25 and 0.75 mg/L for the majority of both experiments.

Anions

Cl^-. The chloride concentration in IEBS-1 is ~32 mg/L at week 1, decreases to ~18 mg/L by week three, and stays around the same value for the run duration. The [Cl^-] in IEBS-2 follows a similar patterns: chloride decreases from ~22 mg/L to ~16 mg/L from week 1 to week 3, and next remains constant for the rest of the experiment..

SO_4^{2-}. The sulfate in both IEBS-1 and IEBS-2 follows the same trend as the chloride concentration. In both experiments, the [SO_4^{2-}] decreases from week 1 to week 3, and then remains relatively constant for the remaining 3 weeks. The sulfate concentrations in IEBS-1 and IEBS-2 range from ~200 to 170 mg/L and 350 to 200 mg/L, respectively. The solutions from IEBS-1 and IEBS-2 were characterized by a strong sulfur smell.

3.2.2 XRD Patterns

The reaction products from both experiments (IEBS-1, IEBS-2) have similar XRD peak patterns (Figure 3). The main peaks correspond to quartz, feldspar (albite, anorthite), and muscovite. There are no obvious differences in peak height or location in the XRD results from the two experiments.

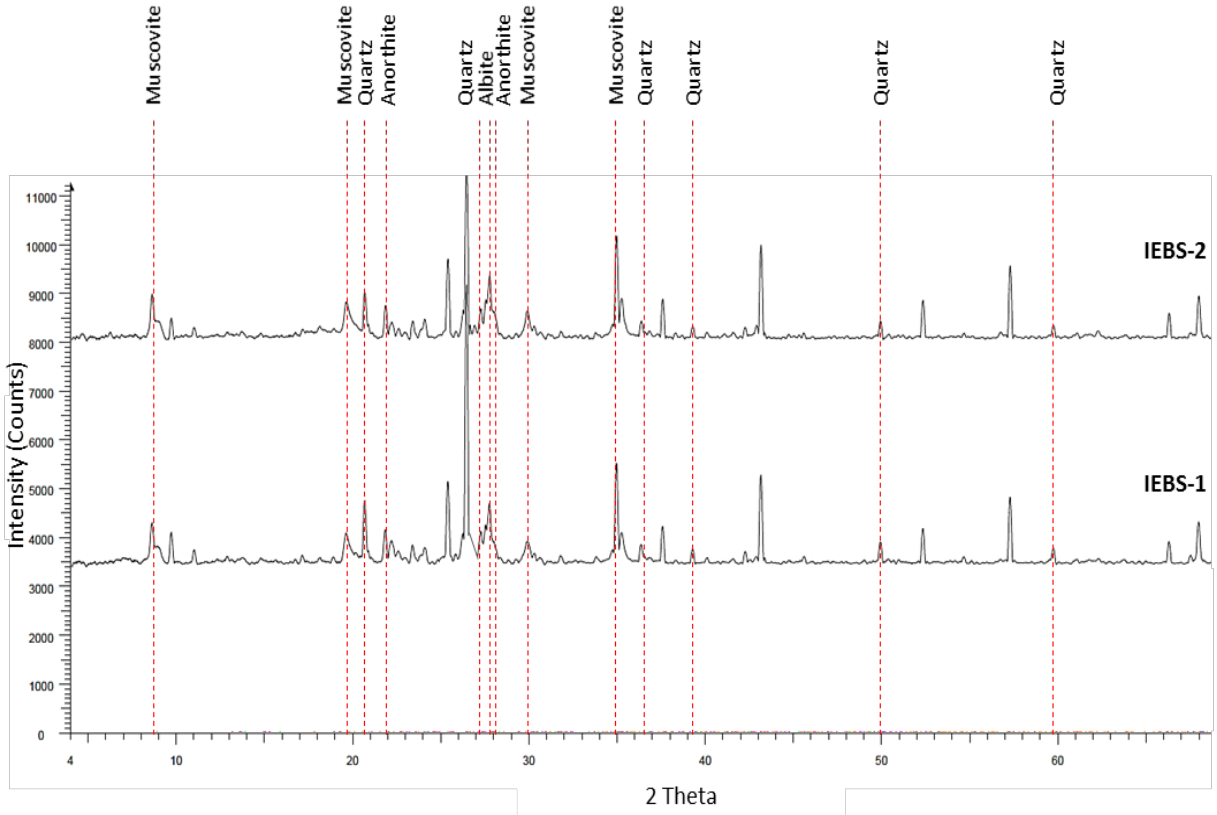

Figure 3. XRD pattern for IEBS-1 and the IEBS-2. The peaks are labeled to their corresponding minerals and unmarked peaks belong to the corundum standard.

3.2.3 QXRD Results

The QXRD results for IEBS-1 and IEBS-2, compared to the starting Wyoming bentonite and Grimsel Granodiorite, are reported in Table 5. The QXRD results show some major differences from the XRD peak patterns and are discussed below.

IEBS-1. The QXRD results from experiment IEBS-1 report smectite, feldspar (orthoclase, albite), muscovite, and quartz. Anorthite, which was observed in the XRD results, is

not present in the QXRD data. In addition, both smectite and muscovite as observed in the QXRD results, whereas only muscovite was recognized in the XRD peak patterns.

IEBS-2. The QXRD results from the IEBS-2 reaction products include feldspar (orthoclase, albite, anorthite), muscovite, and quartz. Orthoclase was not observed in the XRD peak results.

Table 5**:** Quantitative X-Ray Diffraction (QXRD) analyses of the buffer clay (Wyoming Bentonite) the wall rock (Grimsel Granodiorite) and product results of experiments IEBS-1 to IEBS-2. Values are in weight percent, ***b.d.l****. = below detection limit,* * represents data set was normalized to 100.0, (+) represents material detectable but below 0.5 wt. %.

	Wyoming Bentonite	**BG-C-49-1 Granite**	**IEBS-1 Bentonite only**	**IEBS-2 316 SS**
			6 weeks 250°C	**6 weeks 250°C**
Analcime / Wairakite	b.d.l.			
Clinoptilolite	12.0			
Smectite	66.4		11.73	
Kaolinite	b.d.l.			
Albite		25.14	14.81	4.87
Plagioclase	8.3			
Orthoclase		30.84	19.51	9.47
Anorthite				43.55
K-Feldspar	b.d.l.			
Biotite	2.8			
Muscovite			28.02	23.68
Chlorite	b.d.l.			
Calcite	5.5			
Dolomite	+			
Quartz	0.9	44.02	26.17	18.68
Cristobalite/ Opal-C	1.8			
Pyrite	0.4			
Siderite	1.8			
Total:	100.0*	100.00	100.24	100.25

3.2.4 SEM/EDS Results

Reaction products, including loose powder, epoxy mounts, and thin sections, from the two IEBS experiments were characterized using the scanning electron microscope and qualitative elemental abundances were evaluated using EDS. The SEM images are presented in Appendix D and described below.

The SEM images of IEBS-1 and IEBS-2 reaction products show similar features. In both, montmorillonite clay is observed to transition to smectite (Figure D-1A, B; D-4A, B). Spherical crystals are embedded in the fine-grained clay matrix (Figure D-1C, D, E; D-2C, D; D-3A, C; D-4B, C, D, E; D-6B, C). The EDS analyses of these crystals reveal large Ca peaks, with smaller Si, Al, C, and F peaks. The composition of these unknown phases is discussed further in the next section (3.2.5 Electron Microprobe Results). The unknown Ca-phase is more abundant in IEBS-2 than IEBS-1 (Figure 4).

Feldspar surfaces are observed to be variably corroded (Figure D-1F). Glass shards (clinoptilolite) that have a “fishbone” morphology and are preserved in both reaction products (Figure 4).

Images of the 316 SS coupons from IEBS-2 (IEBS-2-steel) show two layers of mineral growth that formed perpendicular to the steel surface (Figure 4). Fe-saponite forms directly adjacent to the pitted steel surface (~30 μm) (Figure D-6A) and chlorite is observed to form a thin layer outside of the Fe-saponite (~7 μm) (Figure 4). Sulfide minerals, such as pyrrhotite are also observed (Figure D-6A).

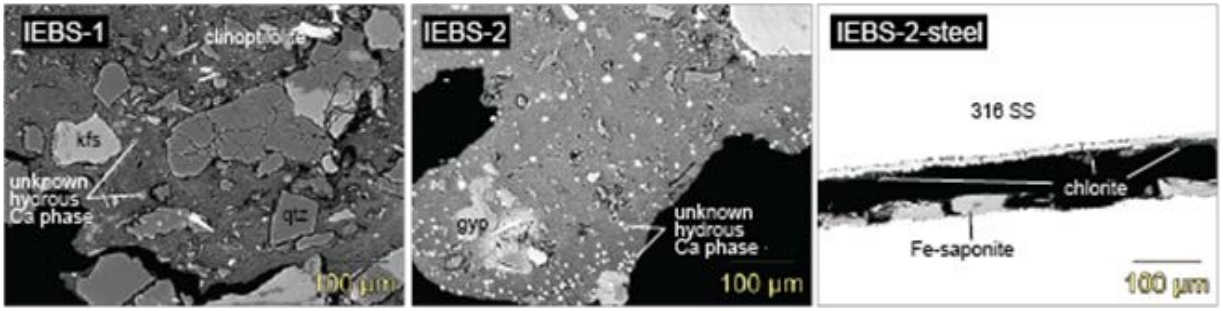

Figure 4. Backscattered electron images of thin sections of IEBS-1 and IEBS-2 reaction products and post-reaction polished 316 SS coupons. Abbreviations: gyp, gypsum; kfs, K-Feldspar; qtz, quartz.

3.2.5 Electron Microprobe Results

Reactions products from IEBS-1, IEBS-2, and IEBS-2-steel were analyzed via electron microprobe (EMP) to determine the major element composition of mineral phases. The EMP analyses primarily targeted the clay matrix, steel alteration products, altered glass shards, and other authigenic minerals. The EMP results are reported in Appendix C and described below.

Clay matrix. The fine-grained groundmass of the reaction products of IEBS-1 and IEBS-2 have similar major element compositions. Both contain ~60 wt. % SiO_2, 20 wt. % Al_2O_3, 5-6 wt% FeO and 1-2% MgO, and ~1% of Na_2O, ~0.3 K_2O, 0.2-0.5 wt. % CaO, and 0.2 wt. % F.

Clinoptilolite. Glass shards present in the precursor bentonite clay were altered to the zeolite clinoptilolite. The Si/Al ratios for the clinoptilolite are dominantly between 4 and 6, with the exception of one analysis with Si/Al = 7.5. The Na/(Na+Ca) values range from 0.55 to 0.75 (Figure 5).

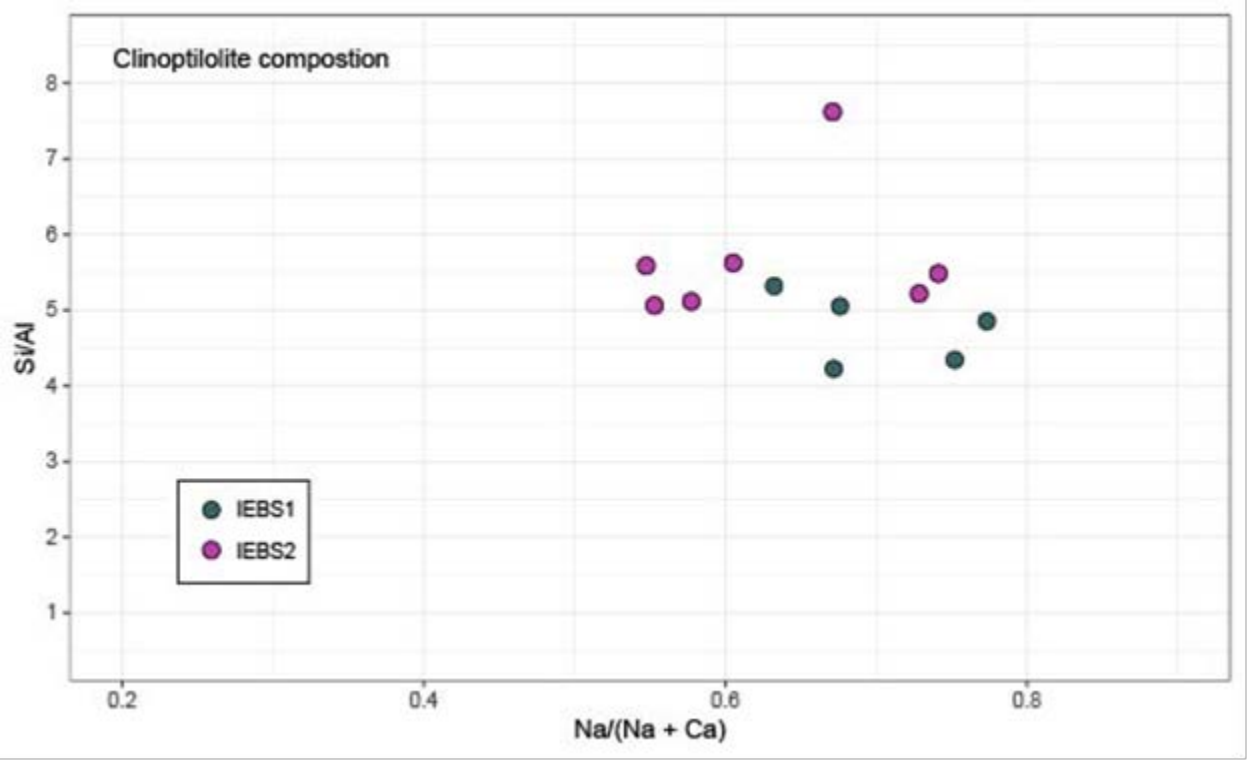

Figure 5. Clinoptilolite compositions in experiments IEBS-1 and IEBS-2 analyzed by EMP.

Calcium (aluminum) silicate hydrates (tobermorite, zeophyllite?). In both IEBS-1 and IEBS-2, <10 μm round mineral grains were observed with the fine-grained matrix. The grains in IEBS-1 were too small to analyze, but some grains in IEBS-2 were large enough to

target. However, the small size and beam sensitivity of this mineral made obtaining EMP analyses difficult. The collected data indicate low SiO_2 wt. % (~12 wt. %) and Al_2O_3 (~1wt. %) and very high CaO (~48%). The low SiO_2 content may be due to sample decrepidation in the beam line prior to SiO_2 analysis. These minerals could be seen actively being destroyed during analysis. Fluorine is present in trace amounts (~0.2–1.2%) Low oxide totals (<60%) indicate the likely presence of H_2O. In addition, EDS analyses demonstrate presence of CO_3. Based on the composition and rounded crystal form, this mineral is likely a calcium (aluminum) silicate hydrate (C(A)SH) and may be identified as mineral zeophyllite ($Ca_4Si_3O_8(OH,F)_4•2(H_2O)$) or tobermorite ($Ca_5Si_6O_{16}(OH)_2•4(H_2O)$), with a small carbonate component.

Steel/Fe alteration. Mineral growth is observed at the surface of the 316 SS coupons in IEBS-2 and around the FeO buffer material in both IEBS-1 and IEBS-2. Fe-saponite is observed to form on the steel interface, and a thin chlorite rim forms outside of the saponite. Stilpnomelane rims the FeO buffer material. The composition of the authigenic Fe-rich minerals is plotted in Figure 6 shows the variation in FeO + MgO wt% versus SiO_2 wt% for these alteration minerals.

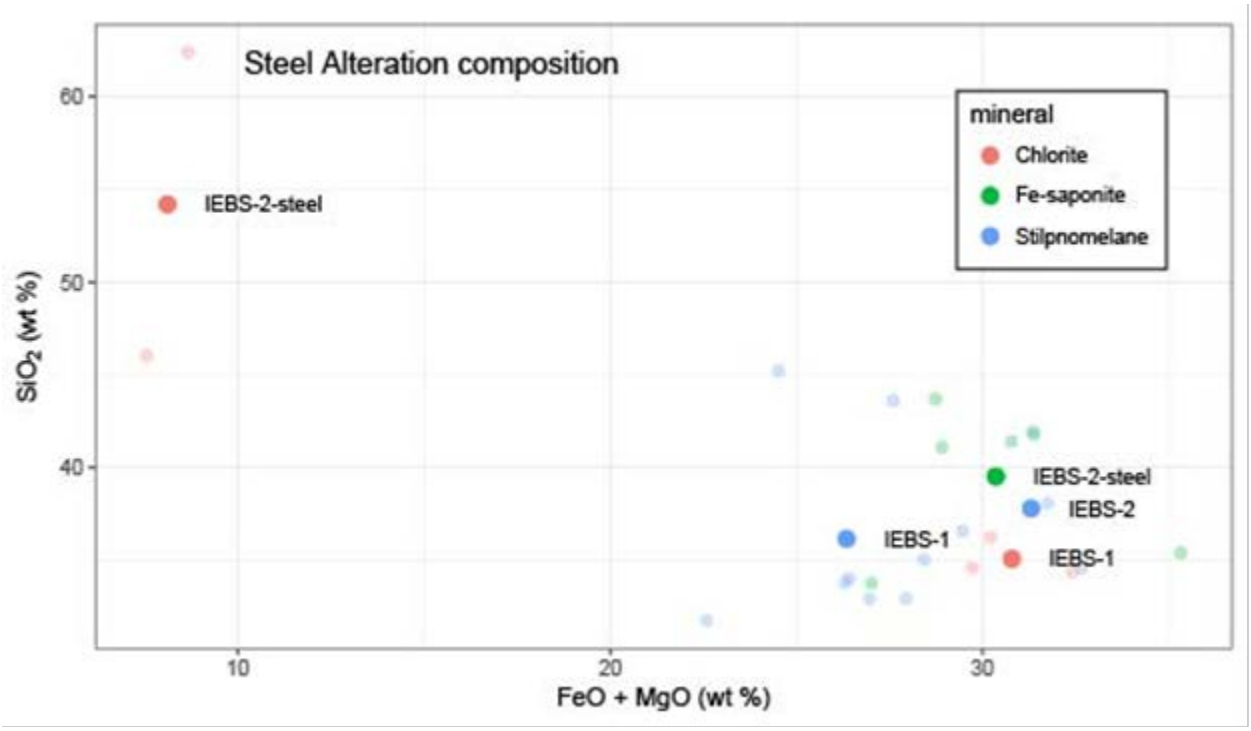

Figure 6. Variation in wt. % FeO and MgO vs. SiO_2. Each point corresponds to a single analysis, and the bold points correspond to averages for all data from each experiment.

4. DISCUSSION

4.1 Grimsel Granodiorite interactions with Wyoming Bentonite

The reaction products formed in the two IEBS experiments include a fine-grained, recrystallized clay matrix with variably altered phenocrysts derived from the starting Grimsel Granodiorite and Wyoming Bentonite, such as feldspars, micas, and quartz. Other authigenic minerals include calcite, quartz, gypsum, and a C(A)SH phase. The following describes our preliminary observations on hydrothermal mineralization and alteration in the IEBS experiments.
Phyllosilicate minerals. SEM imaging of loose powder mounts of the IEBS reaction products show fine-grained clay transitioning to foily phyllosilicate minerals (sericite?) (e.g., Figure D-1A). In addition, the QXRD and XRD analyses of the reaction products show the presence of mixed muscovite and smectite. However, the clay matrix is too fine grained for individual mineral identification. The EMP analyses from the clay matrix of both IEBS-1 and IEBS-2 have very similar compositions (Appendix C). The high silica content of the matrix (~60%) may suggest that fine-grained quartz is interlayered with the phyllosilicate minerals. In terms of alkali elements, the matrix is most enriched in Na (0.15–0.17 atoms per formula unit) in comparison to K (0.02–0.03 apfu) and Ca (0.02–0.03 apfu). The bulk chemistry of the starting materials (i.e., Na-montmorillonite in the Wyoming Bentonite) may prevent illitization due to low K+ in the system. This is a similar result to our previous experimental work with Wyoming Bentonite ± Opalinus Clay, in which illitization was prohibited by the bulk chemistry of the system (Cheshire, et al, 2014)

Feldspars.
Low temperature authigenic feldspars have been identified in both experimental runs; however, further characterization is needed in future experiments to understand their significance.

Calcium (aluminum) silicate hydrates.
In both experiments with Grimsel Granodiorite and Wyoming Bentonite, spherical, C(A)SH phases formed within the fine-grained clay matrix. Small amounts of this mineral are observed in IEBS-1, and it is abundant in IEBS-2 (Figure 4). Based on the composition of this mineral

(Appendix C), it is likely a hydrated calcium silicate, such as zeophyllite ($Ca4Si_3O_8(OH,F)_4•2(H_2O)$) or tobermorite ($Ca_5Si_6O_{16}(OH)_2•4(H_2O)$).

The formation of C(A)SH minerals contrasts with the products of previous experiments with Wyoming Bentonite ± Opalinus Clay host rock. In these experiments, zeolites (analcime–wairakite solid solution) formed, that have similar morphologies and textural contexts. However, the EMP analyses of the spherical minerals formed in the IEBS experiments had significantly lower SiO_2 and Al_2O_3 content and very high CaO. Very Ca-rich minerals, such as tobermorite, have been observed in experiments involving bentonite and cement with highly alkaline bulk chemistries and pH > ~10 (Savage et al., 2007). In comparison, the solution pH over the course of the IEBS experiments did not exceed ~7 (Figure 2) and the experiments did not involve cement. Future investigations will focus on why C(A)SH minerals formed instead of zeolites in the IEBS experiments with Grimsel Granodiorite and Wyoming Bentonite.

H_2S Generation.

The IEBS experiments were accompanied by strong $H_2S_{(aq,g)}$ smells during the course of the 250 °C experiments. The $H_2S_{(aq,g)}$ is most likely related to pyrite solubility from the starting Wyoming Bentonite in a chloride-bearing solution (Crerar et al. 1978; Ohmoto et al. 1994) and the sulfate concentration in the synthetic Grimsel groundwater solution. The reducing nature of the experimental system easily preserved the H2S(aq,g) species. Pyrite contents obtained by QXRD analyses for the Colony Wyoming bentonite (0.4 wt %) are listed in Table 5. Grimsel Granodiorite lacks pyrite, but the synthetic Grimsel groundwater contains appreciable SO_4^{2-} (Table 4). Sulfide-induced corrosion of the waste canisters is the primary concern for the Swedish repository systems (Börjesson et al. 2010), therefore the Swedish Nuclear Fuel and Waste Management Company (SKB) have emplaced fairly strict sulfur specifications (sulfide content < 0.5 wt. %; total sulfur < 1 wt. %) for the bentonite buffer used in their repositories (Börjesson et al. 2010).

pH effects.

In both IEBS experiments, the solution starts with a pH of 7.5 and ends ~6. In IEBS-2, the pH drops to ~5 in the middle of the 6 week experiment (Figure 2). Many of the mineral-forming reactions described above are strongly influenced by the pH of the system. Most mineral reaction

rates that are of concern to a repository are increased under high pH systems. Chermak (1992) showed that under pH conditions of 11–13, Na-rectorite was formed at 150–200 °C within 17 days. Fully formed Na-mica (paragonite) developed after 32 days. Work from Eberl and Hower (1977) and Eberl (1978) do not show illitization until 260–400 °C at quenched pH's ranging from 4–5. These observations are consistent with the current IEBS research; illitization was not observed and Na-rich phyllosilicates formed.

The formation of C(A)SH minerals may also affect the pH of the system. Savage et al. (2002) describe the formation of tobermorite with the generalized reaction:

$$\mathbf{Ca^{2+} + SiO_{2(aq)} + H_2O \rightarrow tobermorite + H^+}$$

in which H^+ is produced. Thus, the formation of C(A)SH minerals, such as tobermorite, may buffer the solution to lower pH values. Savage (1997) reported that zeolite formation within bentonite in contact with cement occurs at lower pH values and C(A)SH mineral formation is favored at high pH (> 11.5). In the IEBS experiments C(A)SH minerals formed, but solution pH values remained below ~7 for the duration of the run. The formation of C(A)SH minerals at low pH (<7) in the IEBS experiments is at odds with previous experiments, and will be the subject of our future investigations.

4.2 Steel interface mineralization

The following mineral phases have been previously identified (Caporuscio et al., 2014) as growing at the interface between bentonite backfill and various steels: Fe-saponite ($(Ca/2,Na)_3(Fe^{++})_3(Si,Al)_4O_{10}(OH)_2$, pentlandite ($(Fe,Ni)_9S_8$) (Figure 5), chromite ($Fe^{++}Cr_2O_4$), pyrrhotite (FeS), millerite (NiS). We have just recently identified another interface material: stilpnomelane (Figure 7). This Fe-bearing phase occurs in IEBS mantling iron metal (one of our solid buffer materials).

Although stilpnomelane is a common metamorphic mineral and occurs over a wide P, T spectra (Winkler, 1976) there is a dearth of occurrences reported in experimental literature. Similar experimental work by Ferrage (2011), Mosser-Ruck et al. (2010), Guillaume et al. (2003) and Meunier et al. (1998) do not report this mineral phase in their reaction products. The chemical formula of stilpnomelane [$K\ (Fe^{++},Mg,\ Fe^{+++})_8(Si,Al)_{12}(O,OH)_{27}$] indicates that iron occurs in

both oxidation states. Given that the iron metal in our experiments (Figure 7) is mantled first by an iron oxide (magnetite?), followed by an Fe sulfide (pyrrhotite) and finally by stilpnomelane, there is a potential that micro-domains of differing oxygen fugacity may be at play. This phenomena and mineral genesis deserves further investigation concerning iron corrosion.

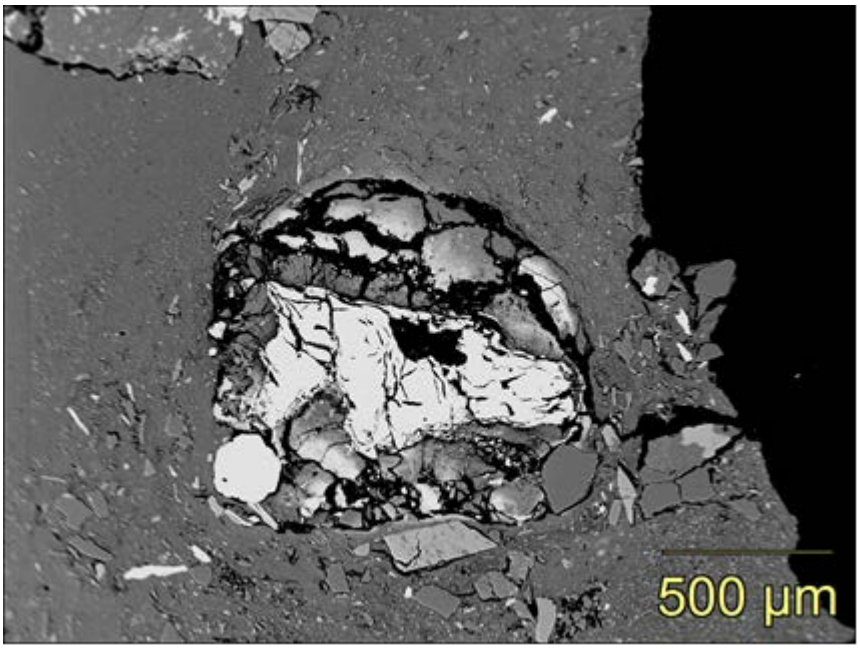

Figure 7. BSE image of iron metal with concentric alteration zones from IEBS-1. Bright white core is remnant iron metal, dark grey is iron oxide, remaining mottled intermediate grey is stilpnomelane.

4.2.1 Steel/bentonite interface reactions

Results from these experiments have shown the more dynamic environment associated with this system is at the bentonite-metal interface. Fe-rich phyllosilicates (i.e., trioctahedral, Fe-rich saponite and chlorite) are crystallized on steel surfaces forming a reactive substrate with a high surface area compared to the original steel surfaces. It is evident that the formation of these surface bound minerals is from the direct crystallization from solution in the localized environments surrounding the metal plates. The reaction is stylized in Figure 8. However, it is uncertain to what extent these authigenic minerals will have an effect on the repository system.

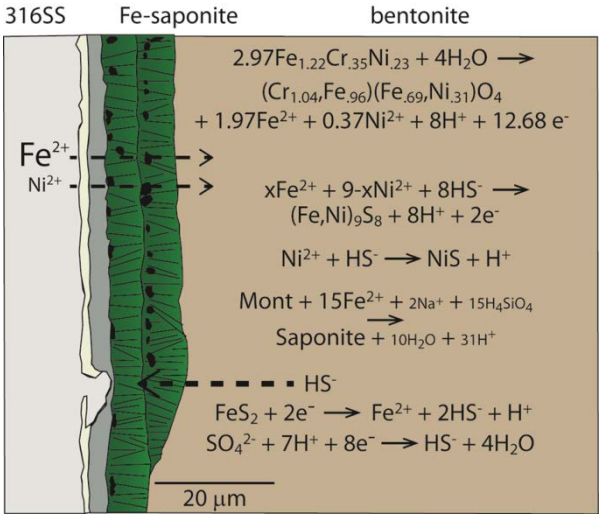

Figure 8. A stylized representation of phyllosilicate mineral growth at the steel interface. Of particular interest is the reaction Montmorillonite → Fe-saponite.

Synthetic Fe-saponites have been crystallized in dilute solutions and gels of silica, Fe-, Al-chlorides at temperatures up to 850 °C and pH of 8.5–9.5 (Kloprogge et al. 1999). This is consistent with a partial dissolution of the steel plates contributing ferrous iron into a fluid phase with silica and aluminum, thereby facilitating Fe-saponite (smectite) crystallization with the steel surfaces acting as a growth substrate. Further, Fe-saponite alteration into chlorite has been suggested (Mosser-Ruck et al., 2010) in the presence of ferrous iron at temperatures approaching 300 °C and near-neutral pH. This was confirmed by Mosser-Ruck et al (2016) through long duration experiments (up to 9 years).The authors were able to demonstrate that smectite is consumed by dissolution to produce chlorite (chamosite) by precipitation. Mosser-Ruck et al. (2016) depicts this reaction by:

3 smectite + 3 Fe +4H_2O → 1 chlorite + 3 quartz + 2 albite +3H_2 + zeolite

Furthermore, we were able to gather microprobe analyses (Appendix C) and images indicating chlorite grows in contact with the steel (where Si is relatively deficient) and then Fe-saponite with a higher Si content (Figure 8).

The stainless steel interaction with bentonite via congruent dissolution/oxidation can be detailed by the following reactions.

Stainless steel dissolution

$Fe_{1.22}Cr_{0.37}Ni_{0.22} \rightarrow 1.22Fe^{2+} + 0.37Cr^{3+} + 0.22Ni^{2+} + 3.99e^{-}$

Smectite evolution

$Fe^{2+} + Ni^{2+} + Cr^{3+} + H_2S_{(aq)} + (Na,K,Ca)_{0.33}(Al_{1.67},Fe^{3+}_{0.20},Mg_{0.13})Si_4O_{10}(OH)_2 \rightarrow (Fe,Ni,Cr)_9S_8 +$

Smectite pentlandite

$(Na, K, Ca)_{0.33}\,Fe_3(Si_{3.67},Al_{0.33})O_{10}(OH)_2$

Fe Saponite

The mechanisms and rates of stainless steel dissolution will be an area of future study. In addition, future IEBS experiments will involve other types of stainless steel (304 SS, LCS).

4.3 International EBS

Outreach to other international programs based at Mont Terri (NAGRA), Grimsel (NAGRA), Stripa (EBS-TF), and perhaps Japan and South Korea will be coordinated with the DOE international program lead (Jens Birkholzer) and lab representatives (Carlos Jove Colon and Liange Zheng). The intent is to share our experimental results in both Argillite and Crystalline rock EBS platforms with international government entities. This will entail correspondence, travel to their research sites (URLs), international workshops, conferences, and cooperative research. We will make a concerted effort to attend the Clay Club meeting, the Hot Bent working group, and the International Engineered Barrier System (Euroclay 2019) conference. At these meetings we will discuss our experimental results and the ramifications of understanding total EBS chemistry, including wall rock-bentonite-steel interactions.

5. CONCLUSION

There have been a large number of investigations on bentonite stability under various repository conditions (Madsen, 1998; Meunier et al., 1998; Guillaume et al., 2003; Guillaume et al., 2004; Mosser-Ruck et al., 2010; Ferrage et al., 2011). Yet, there remain questions regarding bentonite's overall stability and more importantly whether montmorillonite will remain relatively unaltered through the repository life-time.

After initial used-fuel emplacement there will be a pulse of heat flowing into the bentonite buffer producing an environment in which montmorillonite is typically not stable. It would be expected during the early stages of canister emplacement that silica saturation and exchange reactions will take place. However, the relatively dry environment would significantly restrict the mineral reactions due to the limited ion mobility and early saturation. As temperatures increase to peak temperature (currently unknown and will be determined during repository design), various possible zeolite reactions (mordenite, laumontite, analcime, wairakite formation) have the potential to occur if repository conditions shift to the zeolite metamorphic facies (typically starts at 50–150 °C; 100–500 bars). These zeolite reactions, along with silica saturation reactions, will control the pore water solution chemistry and determine any further mineral alteration. Illite formation can still progress, if a K-source is available, but, K-source stability with respect to the repository conditions will determine the illitization rates. It is expected that the initial heat pulse should start to decay after about 100 to 1,000 years (Wersin et al., 2007). After the high temperature pulse passes and temperatures begin to decrease, retrograde reaction have the potential to further change the high temperature mineralogy. As observed in current work, no significant retrograde reactions took place, but as with any experimental work slow kinetics of such reactions make them difficult to show experimentally. It would be expected silica saturation is maintained at continuing lower temperatures by releasing silica from solution, cementing the bentonite. Retrograde zeolite reactions are expected, but currently the extent of such reaction and types are unknown.

There have been a number of similar investigations on bentonite stability under various repository conditions and in contact with various metals replicating possible canister compositions (Guillaume et al., 2003; Guillaume et al., 2004; Wilson et al., 2006; Mosser-Ruck et al., 2010; Ferrage et al., 2011, Mosser-Ruck et al., 2016). Partial dissolution of the steel plates contributing ferrous iron into a fluid phase with silica and aluminum facilitates Fe-saponite

(smectite) crystallization. Bentonite not in contact with the steel waste container does not show the formation of these Fe-rich phyllosilicates. The occurrence of Fe-rich phyllosilicates most likely will not form in the bentonite away from the waste container because there is a low abundance of iron in the system. There are two possible scenarios for Fe-saponite formation: 1) direct crystallization in a Fe- and Si-rich solution as a result from bulk mineralogy influences or 2) Fe^{++} montmorillonite interactions breaking down montmorillonite and producing Fe-saponite. The latter mechanism would be a deleterious reaction to the overall repository as montmorillonite is primary mineral in the barrier.

In this work, we consider the impact host rock (i.e., Grimsel Granodiorite from Switzerland) will have on the bentonite barrier. Several mineral alterations were observed in the heating of Grimsel Granodiorite. The primary mineral reaction is the retention of clinoptilolite in volcanic glass shards and formation of a calcium (aluminum) silicate hydrate (C(A)SH) mineral (tobermorite, zeophyllite?) in the Wyoming Bentonite. Interpreting clay mineral evolution within Grimsel materials is complicated due to the variety of clay minerals present in the Grimsel experimental systems. It does appear that muscovite genesis does occur within the bentonite fraction in the mixed reactions at the current experimental conditions. With any of these experiments representing repository system, kinetics is always an issue that has to be taken into account when interpreting data.

This document summarizes the EBS Grimsel Granodiorite wall rock experiments IEBS-1 and IEBS-2 and attempts to compile pertinent 1) SEM images, 2) XRD (QXRD and clay determination) analyses, 3) electron microprobe data for major mineral phases, and 4) aqueous geochemistry data from both starting materials and the two experiments conducted so far. Concepts developed so far include:

1) Illitization of smectites may be restricted due to the bulk chemistry of the overall system,
2) The interface between bentonite and steel develops a well characterized new mineral phase, Fe-saponite (especially at 300 °C), that grows perpendicular to the steel surface,
3) Another Fe layered phyllosilicate, stilpnomelane, grows in the presence of native iron (one of our solid buffer materials), which alludes to the idea that oxygen fugacity may be quite variable, depending on scale,
4) Zeolites transform as temperature increases. Mine run bentonite contains clinoptilolite, which was preserved in relict glass shards

5) C(A)SH minerals formed within the Wyoming Bentonite mixed with Grimsel Granodiorite
6) No abundant zeolites have been observed
7) Further work to understand formation of C(A)SH minerals at relatively low pH (< 7)

Research needs to be emphasized in the following areas for FY19:

- Continue to build an experimental data base of Grimsel Granodiorite / EBS materials
- Perform transmission electron microscope (TEM) investigation looking at very local chemical changes within a pit corrosion metal surface.
- Corrosion of steels/ interface silicate mantling effect must remain a focus of the upcoming year.
- Incorporate results into Generic modeling codes.

This database, along with summary conclusions will be of use to other experimental teams on the DOE complex, system modeler, and the international repository science community.

6. ACKNOWLEDGEMENTS

We would like to thank George Perkins for water chemistry analyses. Scanning electron microscopy facilities were provided by Materials Science and Technology group at Los Alamos National Laboratory. Dr. Lindsey Hunt at the University of Oklahoma was instrumental in the obtaining of EMP analyses. XRD analyses were performed by Dr. James Maner at University Texas – Austin. Funding was through the Department of Energy's Spent Fuel and Waste Science and Technology.

7. REFERENCES

Aksoyoglu S., Bajo C. & Mantovani M. (1990). Grimsel Test Site: Batch sorption experiments with iodine, bromine, strontium, sodium and cesium on Grimsel mylonite. Nagra Technical Report NTB 91-06; Nagra, Wettingen, Switzerland (February 1991).

Bajo C., Hoehn E., Keil R. & Baeyens B. (1989). Chemical characterization of the groundwater from fault zone AU 96m. In Grimsel test site-laboratory investigations in support of the migration experiments. Nagra Technical Report NTB 88-23; Nagra, Wettingen, Switzerland.

Börjesson, L., Gunnarsson, D., Johannesson, L-E., and Jonsson, E. (2010). Design, production and initial state of the buffer. Svensk Kärnbränslehantering Technical Report, TR-10-15, 89.

Caporuscio, F.A., Cheshire, M.C., Rearick, M.S., and Jove-Colon, C. (2014). LANL argillite EBS experimental program 2014. (FCRD-USED-2014-000491). Los Alamos National Lab. (LANL), Los Alamos, NM (United States).

Chermak, J.A. (1992). Low temperature experimental investigation of the effect of high pH NaOH solutions on the opalinus shale, Switzerland. *Clays and Clay Minerals*, 40, 650-658.

Cheshire, M.C., Caporuscio, F.A., Jove-Colon, C., and McCarney, M.K. (2014) Bentonite Clay Evolution at Elevated Pressures and Temperatures: An experimental study for generic nuclear repositories. *American Mineralogist*, V99, pp. 1662-1675.

Chipera, S.J. and Bish, D.L. (2002). FULLPAT: a full-pattern quantitative analysis program for X-ray powder diffraction using measured and calculated patterns. *Journal of Applied Crystallography*, 35, 744–749.

Crerar, D.A., Susak, N.J., Borcsik, M., and Schwartz, S. (1978). Solubility of the buffer assemblage pyrite + pyrrhotite + magnetite in NaCl solution from 200 to 350 °C. *Geochimica et Cosmochimica Acta*, 42, 1427-1437.

Chung, F.H. (1974). Quantitative interpretations of X-ray diffraction patterns of mixtures. I. Matrix flushing method for quantitative multicomponent analysis. *Journal of Applied Crystallography*, 7, 519-525.

Degueldre C., Pfeiffer H.-R., Alexander W. R., Wernli B. & Bruetsch R. (1996a). Colloid properties in granitic groundwater systems. I: sampling and characterization. *Applied Geochemistry*, 11, 677-695.

Eberl, D. and Hower, J. (1977). The hydrothermal transformation of sodium and potassium smectite into mixed-layer clay. *Clays and Clay Minerals*, 25, 215-227.

Eberl, D. (1978). Reaction series for dioctahedral smectites. *Clays and Clay Minerals*, 26, 327-340.

Eberl, D.D., Velde, B., and McCormick, T. (1993) Synthesis of illite-smectite from smectite at Earth surface temperatures and high pH. *Clay Minerals*, 28, 49-60.

Eikenberg J., Baeyens B. & Bradbury M. H. (1991). The Grimsel Migration Experiment: A hydrogeochemical equilibration test. Nagra Technical Report NTB 90-39; Nagra, Wettingen, Switzerland.

FEBEX (2014). FEBEX-DP Kick-off Meeting. Co-conveners: Gaus, I., Kober, F., Lanyon, G.W. NAGRA, Thun, Switzerland, June 10, 2014, 66 pp.

Ferrage, E., Vidal, O., Mosser-Ruck, R., Cathelineau, M., and Cuadros, J. (2011). A reinvestigation of smectite illitization in experimental hydrothermal conditions: Results from X-ray diffraction and transmission electron microscopy. *American Mineralogist*, 96, 207-223.

Frick U., Alexander W. R., Baeyens B., Bossart P., Bradbury M. H., Bühler Ch., Eikenberg J., Fierz Th., Heer W., Hoehn E., McKinley I. G. & Smith P. A. (1992). Grimsel test site - The radionuclide migration experiment-Overview of investigations 1985 -1990. Nagra Technical Report NTB 91-04, Nagra, Wettingen, Switzerland.

Grimsel (2017). FEBEX-DP Full-scale Engineered Barrier Experiment – Dismantling Project http://www.grimsel.com/gts-phase-vi/febex-dp/febex-dp-introduction.

Guillaume, D., Neaman, A., Cathelineau, M., Mosser-Ruck, R., Peiffert, C., Abdelmoula, M., Dubessy, J., Villieras, F., Baronnet, A., and Michau, N. (2003). Experimental synthesis of chlorite from smectite at 300 °C in the presence of metallic Fe. *Clay Minerals*, 38, 281-302.

Guillaume, D., Neaman, A., Cathelineau, M., Mosser-Ruck, R., Peiffert, C., Abdelmoula, M., Dubessy, J., Villieras, F., and Michau, N. (2004). Experimental study of the transformation of smectite at 80 to 300 °C in the presence of Fe oxides. *Clay Minerals*, 39, 17-34.

Jové-Colón, C. F., Caporuscio, F. A., Levy, S. S., Sutton, M., Blink, J., Greenberg, H. R., Fratoni, M., Halsey, W. G., Wolery, T. J., Rutqvist, J., et al. (2011). Disposal systems evaluations and tool development - Engineered Barrier System (EBS) Evaluation (Fuel Cycle Research and Development). Sandia National Laboratory, (FCRD-USED-2011-000132), 1-192.

Kloprogge, J.T., Komarneni, S. and Amonette, J.E. (1999). Synthesis of smectite clay minerals: a critical review. *Clays and Clay Minerals*, 47, 529-554

Madsen, F.T. (1998). Clay mineralogical investigations related to nuclear waste disposal. *Clay Minerals*, 33, 109-129.

Meunier, A., Velde, B., and Griffault, L. (1998). The reactivity of bentonites: A Review. An application to clay barrier stability for nuclear waste storage. *Clay Minerals*, 33, 187-196.

Missana T., Fernández V., Gutiérrez M. G., Alonso U. & Mingarro M. (2001). CRR project: Sorption studies final report; Unpubl. CIEMAT internal report CIEMAT/DIAE/ 54431/2/2001, CIEMAT, Madrid, Spain.

Missana, T., & Geckeis, H. (2006). Grimsel Test Site–Investigation Phase V. The CRR Final Project Report Series II: Supporting Laboratory Experiments with Radionuclides and Bentonite Colloids NAGRA Technical Report Series NTB, 03-02.

Moore, D. M. and Reynolds, R.C. (1997). X-ray Diffraction and the identification and analysis of clay minerals. Oxford University Press, New York, New York, 377.

Mosser-Ruck, R., Cathelineau, M., Guillaume, D., Charpentier, D., Rousset, D., Barres, O., and Michau, N. (2010). Effects of temperature, pH, and iron/clay and liquid/clay ratios on experimental conversion of dioctahedral smectite to berthierine, chlorite, vermiculite, or saponite. *Clays and Clay Minerals*, 58, 280-291.

Mosser-Ruck, R., Pignatelli, I., Bourdelle, F., Abdelmoula, M., Odile Barres, O., Guillaume, D., Charpentier, D., Rousset, D., · Cathelineau, M., and Michau, N. (2016). Contribution of long-term hydrothermal experiments for understanding the smectite-to-chlorite conversion in geological environments. *Contributions to Mineralogy and Petrology*, 171, 97-118.

Nutt, M. Voegele, M., Jové-Colón, C.F., Wang, Y., Howard, R., Blink, J., Liu, H.H., Hardin, E., and Jenni, K. (2011). Used fuel disposition campaign disposal research and development road map (Fuel cycle research and development). Sandia National Laboratory, (FCRD-USED-2011-000065), 1-121.

Ohmoto, H., Hayashi, K-I, and Kajisa, Y. (1994). Experimental study of the solubilities of pyrite in NaCl-bearing aqueous solutions at 250-350°C. *Geochimica et Cosmochimica Acta*, 58, 2169-2185.

Pouchou, J.L. and Pichoir, F. (1985) "PAP" (φ-ρ-Z) correction procedure for improved quantitative microanalysis. Microbeam Analysis, Ed. Armstrong, J.T., San Francisco Press, pp. 104-106.

Pusch, R. (1979). Highly compacted sodium bentonite for isolating rock-deposited radioactive waste products. *Nuclear Technology*, 45, 153-157.

Savage, D. (1997). Review of the potential effects of alkaline plume migration from a cementitious repository for radioactive waste. Research & Development Technical Report P60, UK Environment Agency, Bristol, UK.

Savage, D., Noy, D.J., Mihara, M., 2002. Modelling the interaction of bentonite with hyperalkaline fluids. *Applied Geochemistry* 17, 207–223.

Savage, D., Walker, C., Arthur, R., Rochelle, C., Oda, C., and Takase, H. (2007). Alteration of bentonite by hyperalkaline fluids: A review of the role of secondary minerals. *Physics and Chemistry of the Earth*, 32, 287-297.

Seyfried, J.R., Janecky, D.R., and Berndt, M.E. (1987). Rocking autoclaves for hydrothermal experiments II. The flexible reaction-cell system. Hydrothermal Experimental Techniques, Eds. Ulmer, G.C. and Barnes, H.L. John Wiley & Sons, pp. 216 – 239.

Środoń, J. (1980). Precise identification of illite/smectite interstratifications by X-ray powder diffraction. *Clays and Clay Minerals*, 28, 401-411.

Wersin, P., Johnson, L.H., and McKinley, I.G. (2007). Performance of the bentonite barrier at temperatures beyond 100°C: A critical review. *Physics and Chemistry of the Earth*, 32, 780-788.

Wilson, J., Cressey, G., Cressey, B., Cuadros, J., Ragnarsdottir, K. V., Savage, D., and Shibata, M. (2006). The effect of iron on montmorillonite stability.(II) Experimental investigation. *Geochimica et Cosmochimica Acta*, 70(2), 323-336

Winkler, H.G.F. (1976) Petrogenesis of Metamorphic Rocks. Springer-Verlag, New York, 329.

APPENDIX

Appendix A
Methods and Mineral Characterization

a. Experimental Setup

The bentonite used in this experimental work was mined from a reducing horizon in Colony, Wyoming. The bentonite was pulverized and sieved to < 3 mm and used with a free moisture content of ~15.5 wt. %. The groundwater solution was prepared using reagent grade materials dissolved in double deionized water. NaOH and HCl were added to adjust the initial solution pH. This solution was then filtered through a 0.45 μm filter and sparged with He before each experiment. The salt solution was added at 9:1 water:bentonite ratio. Initial components for wall rock experiments have been summarized in Table 1.

A second series of experiments were performed to examine the bentonite system with host rock inclusion. Host-rock experiments focused on Grimsel Granodiorite from the Swiss Underground Research Laboratory located near Grimsel Pass. A portion of the Grimsel Granodiorite was crushed and sieved with 10 mesh (~2 mm). Grimsel Granodiorite to be used in experiments was reconstituted at 80 wt. % -10 mesh and 20 wt. % +10 mesh. Synthetic groundwater was chosen to replicate the groundwater composition that represents Grimsel Granodiorite pore water (Table 2, Missana & Geckeis, 2006). The brine solution was added at 9:1 water: rock ratio.

The redox conditions for each system were buffered using a 1:1 mixture (by mass) of Fe3O4 and Fe° added at 0.07 wt. % of the bentonite mass. Approximately 7 wt. % (of total solids mass) 304 stainless steel (NIST SRM 101 g), and 316 stainless steel (NIST SRM 160b), (provided by Sandia National Laboratory) were added to the experiments to mimic the presence of a waste canister.

Reactants were loaded into a flexible gold and fixed into a 500 mL Gasket Confined Closure reactor (Seyfried et al., 1987). Experiments were pressurized to 150 to 160 bar and were heated isothermally at 250 °C for 4 to 6 weeks. Reaction liquids were extracted during the experiments and analyzed to investigate the aqueous geochemical evolution in relationship to mineralogical alterations. The sampled reaction liquids were split three-ways producing aliquots for unfiltered anion, unfiltered cation, and filtered (0.45 μm syringe filter) cation determination. All aliquots were stored in a refrigerator at 1 °C until analysis. The steel corrosion experiment was conducted in a cold seal reaction vessel. The reactants (Opalinus Clay, 316 LC SS, Opalinus Clay brine, and solid buffers) were loaded into a gold capsule. The water/rock ratio was 2:1.The run was pressurized to 150 bar and heated isothermally at 150 ^{o}C for 8 weeks.

b. Mineral Characterization

Chesapeake Energy Laboratory QXRD

X-ray diffraction (XRD) analyses of experimental materials determined mineral compositions. Each sample was ground with 20 wt. % corundum (Al_2O_3) for quantitative XRD analysis of the bulk rock (Chung, 1974). XRD measurements were conducted with a Siemens D500 diffractometer using Cu-Kα radiation. Data were collected from 2 to 70 °2θ with a 0.02 º2θ step-size and count times of 8 to 12 seconds per step. To better analyze the non-clay and clay fractions, the < 2 μm particles were separated via sedimentation in DI H_2O. An aliquot of the < 2 μm suspension was dropped on a zero-background quartz plate and dried. This oriented mount was X-rayed from 2 to 40 °2θ at 8 to 12 s per step. The oriented mount was then saturated with ethylene glycol in a 60°C oven for 24 hours and XRD analysis was repeated. A portion of the > 2 μm particles was ground with a mortar/pestle, deposited on a zero-background quartz plate, and X-rayed under the same parameters as the bulk powder material. The remaining > 2 μm portion was used for electron microscopy. Mineral identification and unit-cell parameters analysis was performed using Jade© 9.5 X-ray data evaluation program with ICDD PDF-4 database. Quantitative phase analysis (QXRD) was performed using FULLPAT (Chipera and Bish, 2002). Illite-smectite composition of higher-ordered (R1-3) illite-smectites were modeled via ClayStrat+ (developed by Hongji Yuan and David Bish). Expandable component abundances for the disordered illite-smectites were calculated via the Δ°2Θ method (Środoń, 1980; Eberl et al., 1993; Moore and Reynolds, 1997). A regression from calculated data were used to calculate the % expandable (%Exp) component in each untreated and reacted bentonite. The equation is:

$$\%Exp = 973.76 - 323.45\Delta + 38.43\Delta^2 - 1.62\Delta^3$$

(Eberl et al., 1993, Eq. 3, R^2=0.99)

with Δ corresponding to Δ°2Θ between the 002 and 003 peak positions for the oriented, ethylene glycol saturated samples.

University Texas-Austin Geoscience Laboratory QXRD

Samples were milled to a fine powder in a tungsten carbide ring mill. Approximately 0.2 g of 0.3 μm corundum (Buehler) was added to a 1 g aliquot of each sample. The corundum and sample mixtures were homogenized by dry milling in an alumina mortar and pestle. A thin layer of petroleum jelly was applied to a one-inch round glass slide. Homogenized mixtures of corundum

and sample were loaded onto glass slides such to form a thin layer of sample across the entirety of the glass slide. Samples were then loaded into the X-ray diffractometer (XRD) for analysis.

XRD Instrument Type and Scan Conditions

All XRD measurements were made at the University of Texas at Austin using a Bruker D8 Advance. The instrument is equipped with a Cu source and a LynxEye detector. The following optically configuration was used for all scans: 1.0 mm divergence slit at the source and a 3.0 mm slit, an anti-scatter tube, a Ni filter for Kb Cu radiation, and a 2.5° axial soller slit at the detector. The source was run at 45 kV and 40 mA for all scans. All samples were scanned between 4° and 70° 2Θ with a stepsize of 0.01° and a counting time of 1 s per step. Samples were rotated during acquisition to maximize random orientation of phases. Total run time for each sample was two hours.

Scan Processing: QXRD

Post-acquisition processing and quantitative XRD (QXRD) were performed using Bruker's DIFFRACplusBasic Evaluation Package (EVA v.15). EVA was used for background subtraction, Kα2 stripping, scan smoothing, and 2Θ displacement. The reference intensity ratio (RIR) method was used for QXRD. The RIR method uses the most intense peak of corundum as a reference intensity to calculate weight fractions of other phases in a sample. Preferred orientation of phases results in poor-quality QXRD results. Rotation of samples during measurement and the method for loading samples in XRD holders minimized preferred orientation. QXRD results for most samples yielded approximately 18 wt.% corundum, which closely matches the amount of corundum added to the sample.

SEM analyses

Analytical electron microscopy was performed using a FEITM Inspect F scanning electron microscope (SEM). All samples were Au/Pd-coated prior to SEM analysis. Imaging with the SEM was performed using a 5.0 kV accelerating voltage and 1.5 spot size. Energy dispersive X-ray spectroscopy (EDS) was performed at 30 kV and a 3.0 spot size.

SEM analyses

Analytical electron microscopy was performed using a FEITM Inspect F scanning electron microscope (SEM). All samples were Au/Pd-coated prior to SEM analysis. Imaging with the SEM was performed using a 5.0 kV accelerating voltage and 1.5 spot size. Energy dispersive X-ray spectroscopy (EDX) was performed at 30 kV and a 3.0 spot size.

c. Aqueous Geochemical Analyses

Major cations and trace metals were analyzed via inductively coupled plasma-optical emission spectrometry (Perkin Elmer Optima 2100 DV) and inductively coupled plasma-mass spectrometry (Elan 6100) utilizing EPA methods 200.7 and 200.8. Ultra-high purity nitric acid was used in sample and calibration preparation prior to sample analysis. Internal standards (Sc, Ge, Bi, and In) were added to samples and standards to correct for matrix effects. Standard Reference Material (SRM) 1643e Trace Elements in Water was used to check the accuracy of the multi-element calibrations. Inorganic anion samples were analyzed by ion chromatography (IC) following EPA method 300 on a Dionex DX-600 system. Aqueous geochemical results are presented in Appendix B.

Appendix B

Water Chemistry IEBS-1 and IEBS-2

IEBS-1 UNFILTERED

Lab ID	Sample Date	Al	B	Ba	Br	Ca	Cl^-	Cr	F^-	Fe	K	Li	Mg	Mn	Na	NO_3^-	PO_4^{3-}	Si	SiO_2	SO_4^{2-}	Sr	Ti	Zn	TDS	Cation	Anion	Balance
		ppm	ppm	ppm	ppm	ppm	ppm	ppm	ppm	ppm	ppm	ppm	ppm	ppm	ppm	ppm	ppm	ppm	ppm	ppm	ppm	ppm	ppm	ppm	ppm	ppm	
IEBS-1-1 UF	11/22/2017	5.01	4.45	0.07	<0.1	2.23	31.94	0.01	6.69	0.79	2.19	0.05	0.38	<0.006	150.31	<0.1	<0.1	263.31	563.48	201.87	0.02	0.01	<0.104	969	14	6	0.42
IEBS-1-2 UF	11/30/2017	2.94	4.62	0.05	<0.1	1.54	19.92	<0.006	6.37	0.37	2.40	0.05	0.37	<0.006	130.46	<0.1	<0.1	221.33	473.65	199.87	0.01	<0.004	<0.104	843	12	5	0.38
IEBS-1-3 UF	12/7/2017	2.46	4.15	0.04	<0.1	1.29	18.27	<0.006	5.87	0.16	1.81	0.04	0.28	<0.006	124.16	<0.1	<0.1	191.7	410.20	182.39	0.01	<0.004	<0.104	751	11	5	0.38
IEBS-1-4 UF	12/14/2017	2.47	3.95	0.05	<0.1	1.33	18.47	0.01	6.21	0.68	1.61	0.03	<0.02	<0.006	120.74	<0.1	<0.1	294.70	630.66	172.72	0.01	<0.004	<0.104	959	13	5	0.48
IEBS-1-5 UF	12/20/2017	2.59	3.75	0.07	<0.1	0.87	17.88	<0.006	5.78	0.28	1.54	0.03	0.12	<0.006	115.98	<0.1	<0.1	303.02	648.46	182.78	0.01	<0.004	<0.104	980	13	5	0.46
IEBS-1-6 UF	1/5/2018	0.70	2.21	0.11	<0.1	1.67	11.78	0.01	3.27	3.94	<1.122	0.10	0.18	0.01	120.14	<0.1	<0.1	156.72	335.37	98.65	0.01	<0.004	<0.104	578	10	3	0.56

IEBS-1 FILTERED

Lab ID	Sample Date	Al	B	Ba	Ca	Cr	Fe	K	Li	Mg	Mn	Na	Si	SiO_2	Sr	Ti	Zn	TDS	Cation	Anion	Balance
		ppm	ppm	ppm	ppm	ppm	ppm	ppm	ppm	ppm	ppm	ppm	ppm	ppm	ppm	ppm	ppm	ppm	ppm	ppm	
IEBS-1-1 F	11/22/2017	4.65	4.51	0.19	1.89	0.01	0.66	2.35	0.04	0.10	<0.006	156.71	259.45	555.23	0.03	<0.004	<0.104	726	14	0	0.97
IEBS-1-2 F	11/30/2017	2.90	4.35	0.06	1.08	<0.006	0.70	1.97	0.04	<0.02	<0.006	130.81	310.90	665.33	0.01	<0.004	<0.104	807	14	0	0.97
IEBS-1-3 F	12/7/2017	2.60	4.19	0.07	0.92	<0.006	1.71	1.85	0.04	0.09	<0.006	127.94	319.37	683.46	0.01	<0.004	<0.104	823	14	0	0.97
IEBS-1-4 F	12/14/2017	2.63	4.03	0.03	0.86	<0.006	0.21	1.95	0.03	<0.02	<0.006	126.17	310.52	664.52	0.01	<0.004	<0.104	800	14	0	0.97
IEBS-1-5 F	12/20/2017	2.71	3.71	0.06	1.00	<0.006	0.45	1.55	0.03	<0.02	<0.006	119.35	325.59	696.77	0.01	<0.004	<0.104	826	14	0	0.98
IEBS-1-6 F	1/5/2018	0.65	1.99	0.12	1.42	0.01	3.87	<1.122	0.10	0.08	<0.006	122.93	167.30	358.02	0.01	<0.004	<0.104	489	10	0	0.98

IEBS-2 UNFILTERED

Lab ID	Sample Date	Al	B	Ba	Br	Ca	Cl^-	Cr	F^-	Fe	K	Li	Mg	Mn	Na	NO_3^-	PO_4^{3-}	Si	SiO_2	SO_4^{2-}	Sr	Ti	Zn	TDS	Cation	Anion	Balance
		ppm	ppm	ppm	ppm	ppm	ppm	ppm	ppm	ppm	ppm	ppm	ppm	ppm	ppm	ppm	ppm	ppm	ppm	ppm	ppm	ppm	ppm	ppm	ppm	ppm	
IEBS-2-1 UF	3/15/2018	3.21	3.76	0.09	0.21	1.86	23.16	0.01	8.50	0.51	1.68	0.05	0.04	<0.006	128.08	0.56	0.17	316.94	678.26	347.49	0.02	<0.004	<0.104	1198	14	9	0.24
IEBS-2-2 UF	3/22/2018	3.23	3.38	0.08	0.14	2.30	17.33	0.01	5.89	0.43	2.12	0.06	0.30	<0.006	109.71	0.43	0.12	256.43	548.76	242.91	0.02	0.01	<0.104	937	12	6	0.32
IEBS-2-3 UF	3/29/2018	2.65	3.04	0.16	0.16	0.76	15.78	0.01	5.27	0.37	1.64	0.06	<0.02	<0.006	106.63	0.53	0.09	222.10	629.41	197.02	0.01	<0.004	<0.104	964	12	5	0.43
IEBS-2-4 UF	4/5/2018	2.65	2.92	0.08	0.13	0.97	15.69	<0.006	5.71	0.27	1.74	0.05	<0.02	<0.006	105.83	0.20	0.07	305.08	652.86	205.86	0.01	<0.004	<0.104	995	13	5	0.42
IEBS-2-5 UF	4/12/2018	2.59	2.75	0.11	0.13	1.27	15.69	<0.006	6.13	0.87	1.62	0.05	0.14	<0.006	103.29	0.31	0.20	295.38	632.11	207.91	0.01	0.01	<0.104	975	12	5	0.41
IEBS-2-6 UF	4/19/2018	2.61	2.58	0.08	0.19	1.55	15.51	<0.006	6.41	0.20	1.38	0.05	0.14	<0.006	97.69	0.78	0.10	287.69	615.65	196.82	0.01	<0.004	<0.104	942	12	5	0.41
IEBS-2-7 UF	4/20/2018	38.84	1.92	0.48	<0.1	7.12	12.41	0.03	4.54	19.27	2.14	0.14	11.84	0.12	113.08	0.21	0.28	284.97	609.84	143.12	0.16	0.20	0.11	966	19	4	0.67

IEBS-2 FILTERED

Lab ID	Sample Date	Al	B	Ba	Ca	Cr	Fe	K	Li	Mg	Mn	Na	Si	SiO_2	Sr	Ti	Zn	TDS	Cation	Anion	Balance
		ppm	ppm	ppm	ppm	ppm	ppm	ppm	ppm	ppm	ppm	ppm	ppm	ppm	ppm	ppm	ppm	ppm	ppm	ppm	
IEBS-2-1 F	3/15/2018	3.04	3.88	0.06	1.67	0.01	0.35	1.98	0.05	<0.02	<0.006	129.33	321.28	687.55	0.02	<0.004	<0.104	828	14	0	0.97
IEBS-2-2 F	3/22/2018	0.81	1.32	0.34	101.77	<0.006	0.12	100.51	0.25	<0.02	<0.006	1859.73	24.22	51.82	0.53	<0.004	<0.104	2117	89	0	1.00
IEBS-2-2 F (rerun)	3/22/2018	0.78	1.13	0.33	106.57	<0.006	<0.036	104.29	0.25	<0.02	<0.006	1943.18	23.91	51.16	0.53	<0.004	<0.104	2208	93	0	1.00
IEBS-2-3 F	3/29/2018	1.63	3.59	6.16	0.72	<0.006	0.28	3.56	0.06	0.08	<0.006	119.63	227.26	448.57	0.03	<0.004	1.41	586	11	0	0.97
IEBS-2-3 F (rerun)	3/29/2018	1.71	3.64	4.77	0.78	0.01	0.21	2.72	0.05	0.07	<0.006	128.78	209.61	475.30	0.03	<0.004	1.41	619	12	0	0.97
IEBS-2-4 F	4/5/2018	2.55	2.85	0.05	1.24	<0.006	0.15	1.71	0.06	0.07	<0.006	107.87	281.38	602.16	0.01	<0.004	<0.104	719	12	0	0.98
IEBS-2-5 F	4/12/2018	2.63	2.73	0.11	1.19	0.01	0.49	2.09	0.05	0.08	<0.006	104.99	291.42	623.63	0.01	<0.004	<0.104	738	12	0	0.98
IEBS-2-6 F	4/19/2018	2.57	2.60	0.09	0.75	0.01	0.73	1.66	0.05	<0.02	<0.006	101.49	299.68	641.32	0.01	<0.004	<0.104	751	12	0	0.98
IEBS-2-7 F	4/20/2018	0.50	1.89	0.09	0.23	0.01	0.52	<1.122	0.12	0.03	<0.006	96.44	207.15	443.29	0.00	<0.004	<0.104	543	9	0	0.98

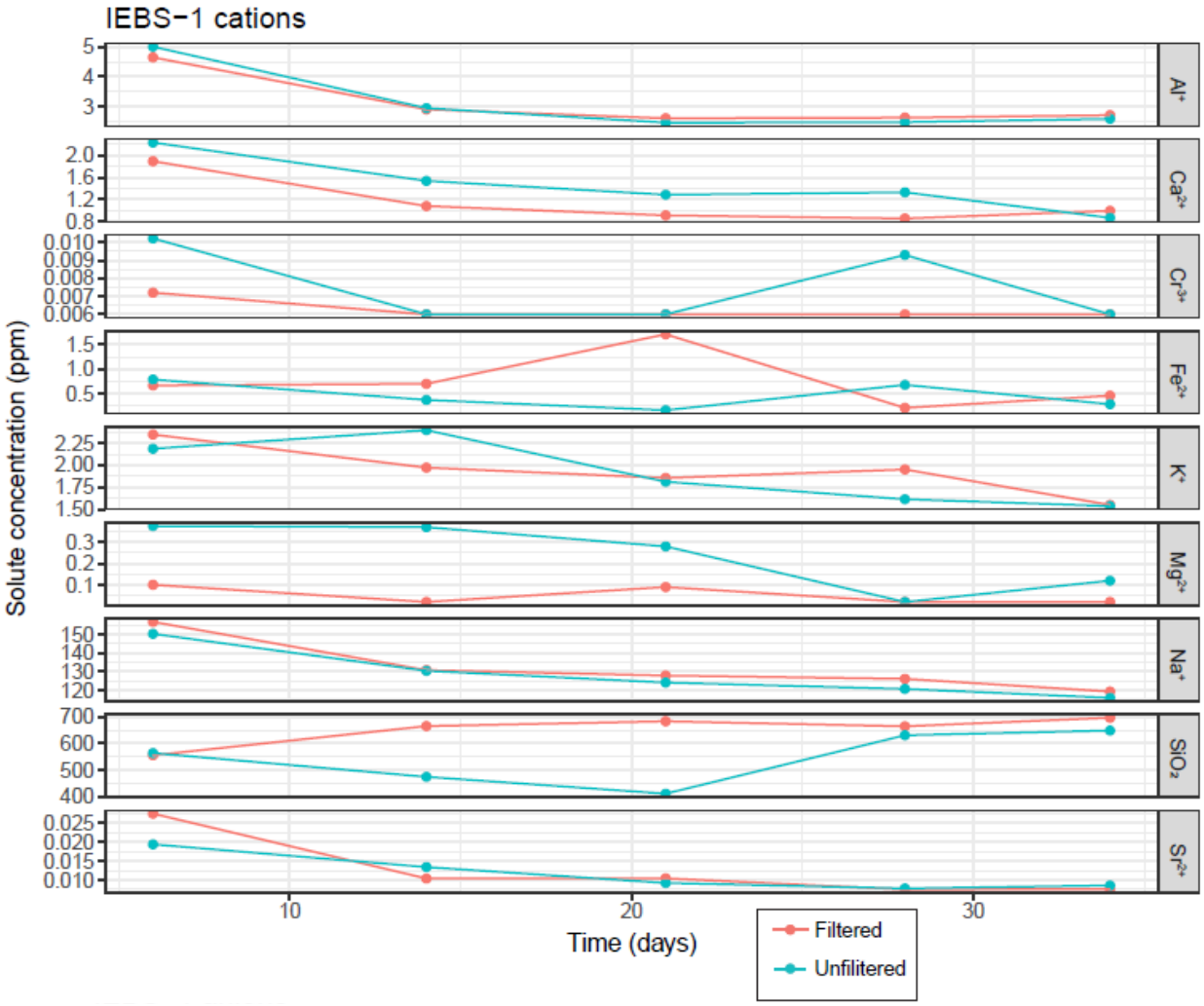
IEBS−1 cations
Solute concentration (ppm)
Al³⁺
Ca²⁺
Cr³⁺
Fe²⁺
K⁺
Mg²⁺
Na⁺
SiO₂
Sr²⁺
Time (days)
Filtered
Unfilitered

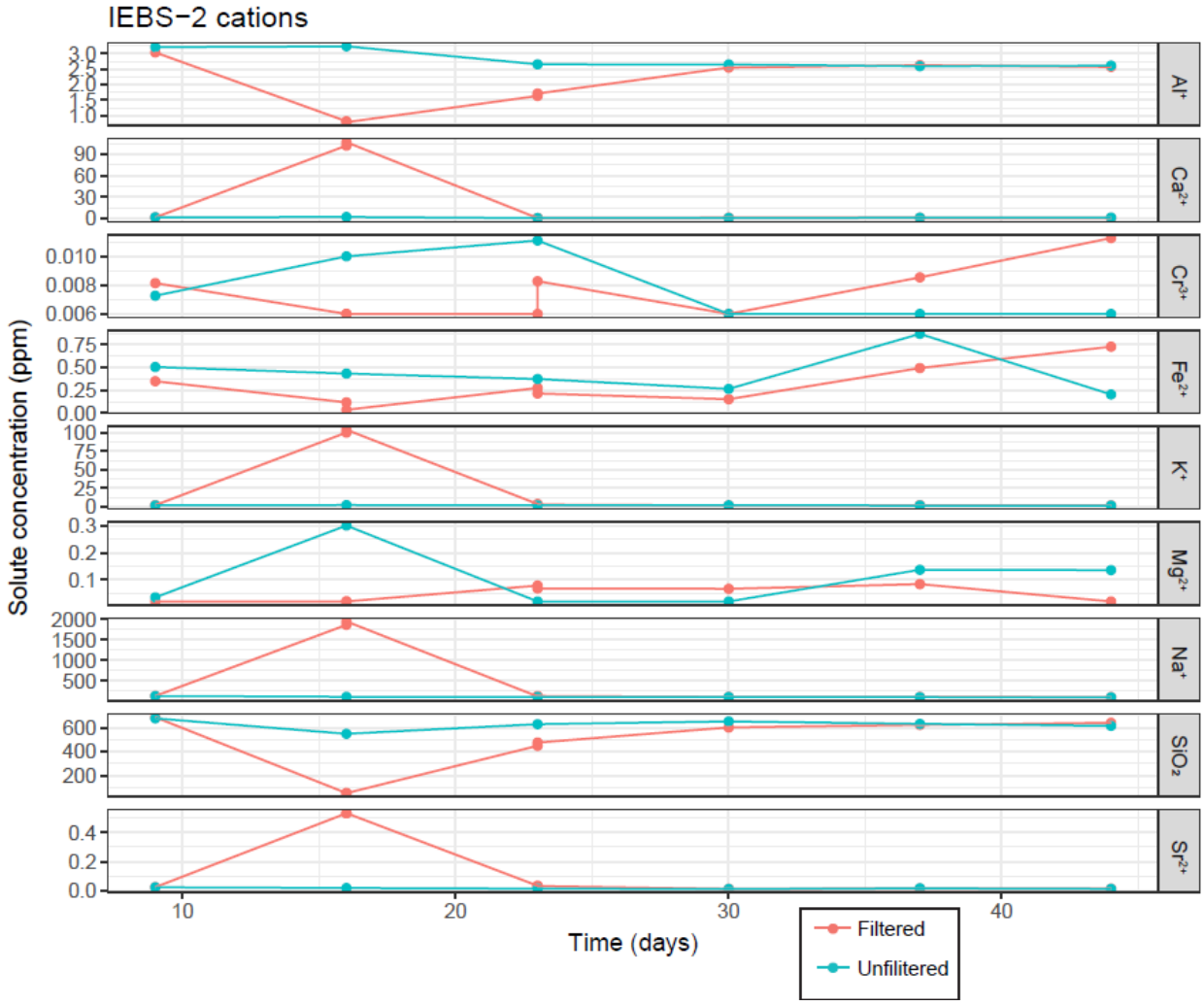
IEBS−2 cations
Solute concentration (ppm)
Al+
Ca2+
Cr3+
Fe2+
K+
Mg2+
Na+
SiO2
Sr2+
Time (days)
Filtered
Unfilitered

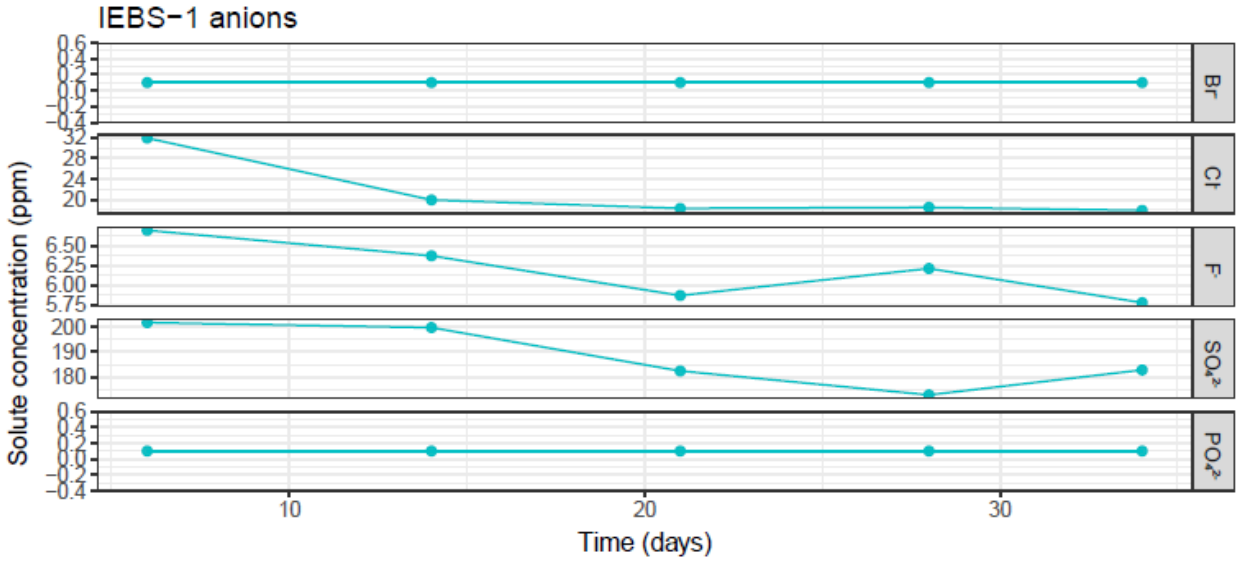
IEBS−1 anions
Solute concentration (ppm)
Br⁻
Cl⁻
F⁻
SO₄²⁻
PO₄³⁻
Time (days)

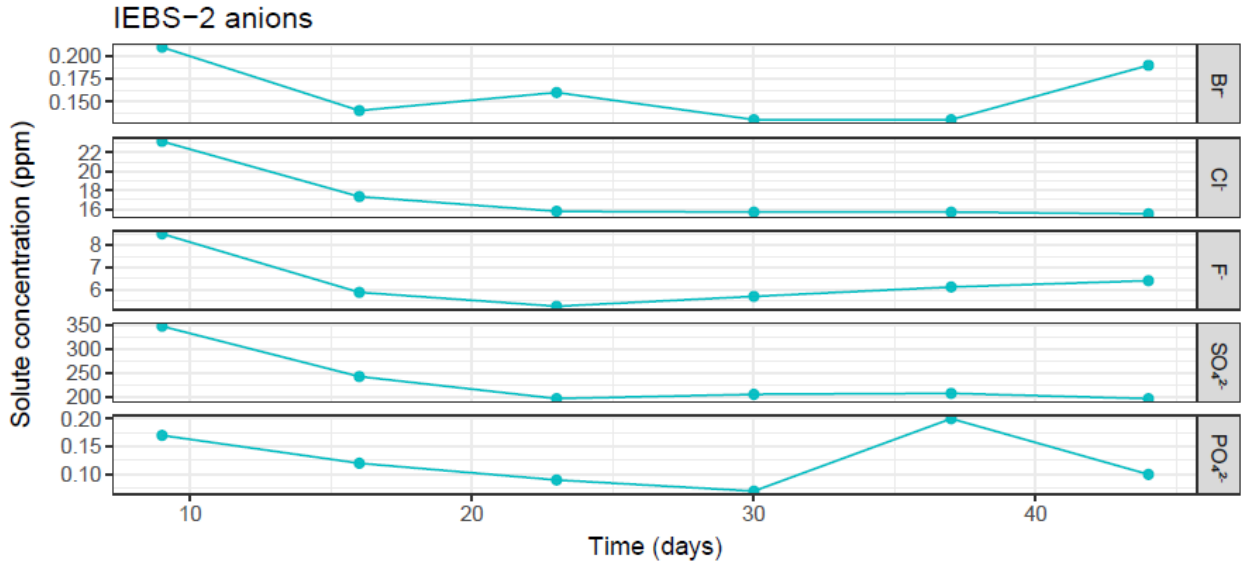
IEBS−2 anions
Solute concentration (ppm)
Br⁻
Cl⁻
F⁻
SO₄²⁻
PO₄³⁻
Time (days)

Appendix C

Electron Microprobe Data IEBS-1 and IEBS-2

Table C-1: EMP standards and oxide detection limits for silicate analyses

Element	Standard Material	Minimum Detection Limit[a]
Mg	Synthetic Phlogopite	0.02
F	Synthetic Phlogopite	0.11
Na	Albite (Amelia, NC, U.S.A, Rutherford Mine)	0.02
Al	Labradorite (Chihuahua, Mexico)	0.02
Si	Labradorite (Chihuahua, Mexico)	0.02
Ca	Labradorite (Chihuahua, Mexico)	0.01
Cl	Tugtupite (Greenland)	0.01
K	Adularia (St. Gotthard, Switzerland)	0.01
Ti	Titanite glass (Penn State)	0.02
Cr	Synthetic Magnesio-chromite	0.04
Mn	Rhodonite (unknown locality)	0.02
Fe	Augite (unknown locality)	0.02
Ni	Synthetic Liebenbergite	0.06
Zn	Gahnite	0.05

[a] Minimum Detection Limit (MDL) values for oxides of respective elements

IEBS-1															
Clinoptilolite	**SiO_2**	**TiO_2**	**Al_2O_3**	**Cr_2O_3**	**FeO**	**NiO**	**MnO**	**MgO**	**CaO**	**Na_2O**	**K_2O**	**Cl**	**F**	**O=F&Cl**	**TOTAL**
IEBS-1 Area 1 Shard	70.70	0.01	11.28	0.00	0.10	0.00	0.01	0.10	1.98	1.89	0.39	0.01	0.02	-0.01	86.47
IEBS-1 Area 3 Shard	62.94	0.01	12.29	0.00	0.09	0.00	0.01	0.13	1.83	3.07	0.45	0.00	0.03	-0.01	80.83
IEBS-1 Area 3 Shard	70.38	0.01	11.82	0.00	0.08	0.01	0.03	0.10	1.88	2.17	0.40	0.00	0.05	-0.02	86.87
IEBS-1 Area 3 Shard	64.94	0.00	11.35	0.00	0.11	0.00	0.04	0.13	1.77	3.34	0.29	0.00	0.02	-0.01	81.96
IEBS-1 Area 4 shard	61.11	0.00	12.28	0.00	0.10	0.00	0.02	0.11	2.03	2.29	0.48	0.00	0.00	0.00	78.42
AVERAGE	**66.02**	**0.00**	**11.80**	**0.00**	**0.10**	**0.00**	**0.02**	**0.11**	**1.90**	**2.55**	**0.40**	**0.00**	**0.03**	**-0.01**	**82.91**
Std. Dev.	**4.35**	**0.00**	**0.48**	**0.00**	**0.01**	**0.01**	**0.01**	**0.01**	**0.11**	**0.62**	**0.08**	**0.00**	**0.02**	**0.01**	**3.66**
	18 oxygen atoms per formula unit (sum excludes F & Cl)														
	Si	**Ti**	**Al**	**Cr**	**Fe**	**Ni**	**Mn**	**Mg**	**Ca**	**Na**	**K**	**Cl**	**F**		**Sum**
IEBS-1 Area 1 Shard	7.676	0.001	1.443	0.000	0.009	0.000	0.000	0.016	0.231	0.397	0.054	0.001	0.008		9.827
IEBS-1 Area 3 Shard	7.399	0.000	1.703	0.000	0.009	0.000	0.001	0.023	0.231	0.700	0.068	0.000	0.012		10.133
IEBS-1 Area 3 Shard	7.619	0.001	1.508	0.000	0.007	0.001	0.002	0.016	0.218	0.455	0.055	0.000	0.018		9.882
IEBS-1 Area 3 Shard	7.513	0.000	1.548	0.000	0.010	0.000	0.004	0.022	0.219	0.748	0.042	0.000	0.009		10.108
IEBS-1 Area 4 shard	7.388	0.000	1.749	0.000	0.010	0.000	0.002	0.019	0.263	0.538	0.074	0.001	0.000		10.043
AVERAGE	**7.52**	**0.00**	**1.59**	**0.00**	**0.01**	**0.00**	**0.00**	**0.02**	**0.23**	**0.57**	**0.06**	**0.00**	**0.01**		**10.00**
Std. Dev.	**0.13**	**0.00**	**0.13**	**0.00**	**0.00**	**0.00**	**0.00**	**0.00**	**0.02**	**0.15**	**0.01**	**0.00**	**0.01**		**0.14**
Chlorite	**SiO_2**	**TiO_2**	**Al_2O_3**	**Cr_2O_3**	**FeO**	**NiO**	**MnO**	**MgO**	**CaO**	**Na_2O**	**K_2O**	**Cl**	**F**	**O=F&Cl**	**TOTAL**
IEBS-1 Area 1 Chlorite	34.60	1.58	16.65	0.00	22.61	0.00	0.60	7.11	0.01	0.16	9.24	0.09	0.72	-0.32	92.64
IEBS-1 Area 3 chlorite	36.26	1.86	16.32	0.00	22.18	0.00	0.57	8.04	0.00	0.17	9.53	0.07	0.80	-0.35	95.00
IEBS-1 Area 4 chlorite	34.40	4.52	14.13	0.00	24.58	0.00	0.28	7.82	0.00	0.41	8.85	0.22	0.54	-0.28	95.21
AVERAGE	**35.09**	**2.65**	**15.70**	**0.00**	**23.12**	**0.00**	**0.48**	**7.66**	**0.01**	**0.25**	**9.21**	**0.13**	**0.69**	**-0.32**	**94.29**
Std. Dev.	**1.02**	**1.62**	**1.37**	**0.00**	**1.28**	**0.00**	**0.18**	**0.49**	**0.00**	**0.14**	**0.34**	**0.08**	**0.14**	**0.04**	**1.43**
	11 oxygen atoms per formula unit (sum excludes F & Cl)														
	Si	**Ti**	**Al**	**Cr**	**Fe**	**Ni**	**Mn**	**Mg**	**Ca**	**Na**	**K**	**Cl**	**F**		**Sum**
IEBS-1 Area 1 Chlorite	2.777	0.095	1.575	0.000	1.517	0.000	0.040	0.850	0.001	0.025	0.946	0.012	0.182		7.826
IEBS-1 Area 3 chlorite	2.768	0.107	1.469	0.000	1.416	0.000	0.037	0.915	0.000	0.025	0.928	0.009	0.193		7.665
IEBS-1 Area 4 chlorite	2.721	0.269	1.317	0.000	1.626	0.000	0.019	0.922	0.000	0.063	0.893	0.029	0.135		7.830
AVERAGE	**2.76**	**0.16**	**1.45**	**0.00**	**1.52**	**0.00**	**0.03**	**0.90**	**0.00**	**0.04**	**0.92**	**0.02**	**0.17**		**7.77**
Std. Dev.	**0.03**	**0.10**	**0.13**	**0.00**	**0.10**	**0.00**	**0.01**	**0.04**	**0.00**	**0.02**	**0.03**	**0.01**	**0.03**		**0.09**
Unknown zeolite pseudomorph	**SiO_2**	**TiO_2**	**Al_2O_3**	**Cr_2O_3**	**FeO**	**NiO**	**MnO**	**MgO**	**CaO**	**Na_2O**	**K_2O**	**Cl**	**F**	**O=F&Cl**	**TOTAL**
IEBS-1 Area 2 Analcime?	46.76	0.13	13.44	0.00	18.93	0.00	0.14	5.24	0.70	2.98	0.22	0.03	0.12	-0.06	88.58

IEBS-1 Area 6 analcime?	42.38	0.09	11.97	0.00	26.47	0.08	0.20	5.83	1.27	6.03	0.26	0.02	0.00	0.00	94.58
AVERAGE	**44.57**	**0.11**	**12.71**	**0.00**	**22.70**	**0.04**	**0.17**	**5.53**	**0.99**	**4.50**	**0.24**	**0.02**	**0.06**	**-0.03**	**91.58**
Std. Dev.	**3.10**	**0.03**	**1.04**	**0.00**	**5.33**	**0.05**	**0.04**	**0.42**	**0.40**	**2.15**	**0.03**	**0.01**	**0.08**	**0.04**	**4.25**
	6 oxygen atoms per formula unit (sum excludes F & Cl)														
	Si	**Ti**	**Al**	**Cr**	**Fe**	**Ni**	**Mn**	**Mg**	**Ca**	**Na**	**K**	**Cl**	**F**		**Sum**
IEBS-1 Area 2 Analcime?	1.935	0.004	0.655	0.000	0.655	0.000	0.005	0.323	0.031	0.239	0.011	0.002	0.015		3.859
IEBS-1 Area 6 analcime?	1.760	0.003	0.586	0.000	0.919	0.003	0.007	0.361	0.057	0.485	0.014	0.001	0.000		4.194
AVERAGE	**1.85**	**0.00**	**0.62**	**0.00**	**0.79**	**0.00**	**0.01**	**0.34**	**0.04**	**0.36**	**0.01**	**0.00**	**0.01**		**4.03**
Std. Dev.	**0.12**	**0.00**	**0.05**	**0.00**	**0.19**	**0.00**	**0.00**	**0.03**	**0.02**	**0.17**	**0.00**	**0.00**	**0.01**		**0.24**
Clay Matrix	**SiO_2**	**TiO_2**	**Al_2O_3**	**Cr_2O_3**	**FeO**	**NiO**	**MnO**	**MgO**	**CaO**	**Na_2O**	**K_2O**	**Cl**	**F**	**O=F&Cl**	**TOTAL**
IEBS-1 Area 4 Matrix	61.55	0.11	21.61	0.00	3.99	0.00	0.01	1.91	0.54	1.11	0.28	0.02	0.20	-0.09	91.14
IEBS-1 Area 4 matrix	59.35	0.12	22.31	0.00	4.17	0.01	0.01	1.90	0.14	0.99	0.27	0.02	0.28	-0.12	89.29
IEBS-1 Area 1 Matrix	59.55	0.12	22.16	0.00	3.93	0.01	0.02	2.08	0.42	1.15	0.27	0.02	0.21	-0.09	89.74
AVERAGE	**60.15**	**0.12**	**22.03**	**0.00**	**4.03**	**0.01**	**0.01**	**1.97**	**0.37**	**1.08**	**0.27**	**0.02**	**0.23**	**-0.10**	**90.06**
Std. Dev.	**1.22**	**0.01**	**0.37**	**0.00**	**0.13**	**0.01**	**0.00**	**0.10**	**0.20**	**0.09**	**0.01**	**0.00**	**0.05**	**0.02**	**0.96**
	12 oxygen atoms per formula unit (sum excludes F & Cl)														
	Si	**Ti**	**Al**	**Cr**	**Fe**	**Ni**	**Mn**	**Mg**	**Ca**	**Na**	**K**	**Cl**	**F**		**Sum**
IEBS-1 Area 4 Matrix	4.341	0.006	1.796	0	0.235	0	6E-04	0.201	0.041	0.152	0.025	0.002	0.045		6.80
IEBS-1 Area 4 matrix	4.268	0.006	1.891	0	0.251	6E-04	6E-04	0.204	0.011	0.138	0.025	0.002	0.064		6.80
IEBS-1 Area 1 Matrix	4.271	0.006	1.873	0	0.236	6E-04	0.001	0.222	0.032	0.16	0.025	0.002	0.048		6.83
AVERAGE	**4.29**	**0.01**	**1.85**	**0.00**	**0.24**	**0.00**	**0.00**	**0.21**	**0.03**	**0.15**	**0.02**	**0.00**	**0.05**		**6.81**
Std. Dev.	**0.04**	**0.00**	**0.05**	**0.00**	**0.01**	**0.00**	**0.00**	**0.01**	**0.02**	**0.01**	**0.00**	**0.00**	**0.01**		**0.02**
Stilpnomelane	**SiO_2**	**TiO_2**	**Al_2O_3**	**Cr_2O_3**	**FeO**	**NiO**	**MnO**	**MgO**	**CaO**	**Na_2O**	**K_2O**	**Cl**	**F**	**O=F&Cl**	**TOTAL**
IEBS-1 Area 5 stil?	33.81	0.02	12.03	0.00	24.99	0.01	0.11	1.31	0.58	1.84	0.08	0.13	0.00	-0.03	74.90
IEBS-1 Area 5 stil?	32.93	0.01	12.39	0.00	25.73	0.02	0.12	1.23	0.75	1.96	0.06	0.09	0.02	-0.03	75.29
IEBS-1 Area 5 stil?	31.76	0.03	11.14	0.01	21.30	0.00	0.11	1.28	0.34	2.02	0.08	0.16	0.05	-0.05	68.21
IEBS-1 Area 5 stil?	43.61	0.09	15.21	0.01	25.60	0.00	0.11	2.00	1.09	2.45	0.15	0.01	0.16	-0.07	90.32
IEBS-1 Area 6 stil?	34.02	0.01	11.09	0.01	24.29	0.00	0.10	2.12	0.48	1.59	0.02	0.10	0.00	-0.02	73.85
IEBS-1 Area 6 stil?	35.03	0.02	12.55	0.00	26.48	0.00	0.10	1.94	0.46	1.78	0.03	0.09	0.05	-0.04	78.49
IEBS-1 Area 6 stil?	32.95	0.02	11.79	0.01	26.36	0.02	0.10	1.59	0.44	1.57	0.04	0.14	0.01	-0.03	75.02
IEBS-1 Area 6 stil?	45.21	0.06	17.01	0.01	22.68	0.00	0.10	1.84	0.96	4.45	0.30	0.02	0.07	-0.03	92.64

AVERAGE	**36.17**	**0.03**	**12.90**	**0.01**	**24.68**	**0.01**	**0.11**	**1.66**	**0.64**	**2.21**	**0.10**	**0.09**	**0.04**	**-0.04**	**78.59**
Std. Dev.	**5.20**	**0.03**	**2.10**	**0.00**	**1.84**	**0.01**	**0.01**	**0.36**	**0.27**	**0.95**	**0.09**	**0.05**	**0.05**	**0.02**	**8.47**
	28 oxygen atoms per formula unit (sum excludes F & Cl)														
	Si	**Ti**	**Al**	**Cr**	**Fe**	**Ni**	**Mn**	**Mg**	**Ca**	**Na**	**K**	**Cl**	**F**		**Sum**
IEBS-1 Area 5 stil?	8.281	0.003	3.472	0.000	5.120	0.002	0.022	0.478	0.151	0.875	0.026	0.052	0.000		18.431
IEBS-1 Area 5 stil?	8.089	0.002	3.586	0.000	5.286	0.004	0.025	0.451	0.196	0.935	0.019	0.036	0.018		18.593
IEBS-1 Area 5 stil?	8.434	0.005	3.486	0.001	4.730	0.000	0.024	0.506	0.096	1.042	0.026	0.070	0.038		18.351
IEBS-1 Area 5 stil?	8.577	0.013	3.526	0.001	4.211	0.000	0.018	0.586	0.229	0.934	0.037	0.005	0.098		18.131
IEBS-1 Area 6 stil?	8.406	0.002	3.230	0.002	5.020	0.000	0.022	0.781	0.128	0.762	0.008	0.042	0.000		18.361
IEBS-1 Area 6 stil?	8.198	0.003	3.462	0.000	5.183	0.001	0.019	0.677	0.114	0.809	0.010	0.037	0.040		18.477
IEBS-1 Area 6 stil?	8.141	0.004	3.434	0.002	5.448	0.003	0.021	0.586	0.116	0.754	0.012	0.059	0.005		18.520
IEBS-1 Area 6 stil?	8.558	0.009	3.794	0.001	3.591	0.000	0.016	0.518	0.194	1.632	0.073	0.007	0.039		18.388
AVERAGE	**8.34**	**0.01**	**3.50**	**0.00**	**4.82**	**0.00**	**0.02**	**0.57**	**0.15**	**0.97**	**0.03**	**0.04**	**0.03**		**18.41**
Std. Dev.	**0.19**	**0.00**	**0.16**	**0.00**	**0.63**	**0.00**	**0.00**	**0.11**	**0.05**	**0.29**	**0.02**	**0.02**	**0.03**		**0.14**

IEBS-2															
C(A)SH (Zeophyllite, tobermorite?)	**SiO_2**	**TiO_2**	**Al_2O_3**	**Cr_2O_3**	**FeO**	**NiO**	**MnO**	**MgO**	**CaO**	**Na_2O**	**K_2O**	**Cl**	**F**	**O=F&Cl**	**TOTAL**
IEBS-2 Area 1 zeolite?	12.11	0.01	1.65	0.00	0.76	0.00	0.06	0.08	46.27	0.28	0.03	0.03	0.69	-0.30	61.28
IEBS-2 Area 1 zeolite?	9.79	0.01	1.88	0.00	0.82	0.00	0.06	0.09	48.20	0.31	0.02	0.02	0.54	-0.23	61.20
IEBS-2 Area 1 zeolite?	7.45	0.01	1.07	0.00	0.66	0.00	0.07	0.08	41.74	0.55	0.02	0.02	0.22	-0.10	51.66
IEBS-2 Area 1 zeolite?	7.27	0.01	1.74	0.00	0.64	0.00	0.08	0.06	42.03	0.38	0.02	0.03	0.57	-0.25	52.26
IEBS-2 Area 1-2 zeolite?	10.13	0.00	1.80	0.00	0.70	0.01	0.04	0.13	48.64	0.43	0.02	0.03	0.94	-0.40	61.93
IEBS-2 Area 1-2 zeolite?	9.33	0.00	1.25	0.00	0.58	0.01	0.05	0.08	48.25	0.49	0.03	0.03	1.24	-0.53	60.11
IEBS-2 Area 1-2 zeolite?	10.45	0.00	3.37	0.00	0.66	0.00	0.03	0.12	43.09	0.74	0.04	0.04	0.80	-0.35	58.52
AVERAGE	**9.50**	**0.01**	**1.82**	**0.00**	**0.69**	**0.00**	**0.05**	**0.09**	**45.46**	**0.45**	**0.03**	**0.03**	**0.71**	**-0.31**	**58.14**
Std. Dev.	**1.70**	**0.00**	**0.74**	**0.00**	**0.08**	**0.00**	**0.02**	**0.02**	**3.09**	**0.16**	**0.01**	**0.01**	**0.32**	**0.14**	**4.36**
	12 oxygen atoms per formula unit (sum excludes F & Cl)														
	Si	**Ti**	**Al**	**Cr**	**Fe**	**Ni**	**Mn**	**Mg**	**Ca**	**Na**	**K**	**Cl**	**F**		**Sum**
IEBS-2 Area 1 zeolite?	1.815	0.001	0.291	0.000	0.095	0.000	0.008	0.018	7.431	0.081	0.006	0.008	0.327		9.747
IEBS-2 Area 1 zeolite?	1.516	0.001	0.343	0.000	0.106	0.000	0.008	0.021	7.998	0.093	0.004	0.005	0.264		10.090
IEBS-2 Area 1 zeolite?	1.407	0.001	0.238	0.000	0.104	0.000	0.011	0.023	8.447	0.201	0.005	0.006	0.131		10.438
IEBS-2 Area 1 zeolite?	1.330	0.001	0.375	0.000	0.098	0.000	0.012	0.016	8.239	0.135	0.005	0.009	0.330		10.212
IEBS-2 Area 1-2 zeolite?	1.523	0.000	0.319	0.000	0.088	0.001	0.005	0.029	7.834	0.125	0.004	0.008	0.447		9.928
IEBS-2 Area 1-2 zeolite?	1.441	0.000	0.228	0.000	0.075	0.001	0.007	0.018	7.985	0.147	0.006	0.008	0.606		9.908
IEBS-2 Area 1-2 zeolite?	1.626	0.000	0.618	0.000	0.086	0.000	0.004	0.028	7.184	0.223	0.008	0.011	0.394		9.776
AVERAGE	**1.52**	**0.00**	**0.34**	**0.00**	**0.09**	**0.00**	**0.01**	**0.02**	**7.87**	**0.14**	**0.01**	**0.01**	**0.36**		**10.01**
Std. Dev.	**0.16**	**0.00**	**0.13**	**0.00**	**0.01**	**0.00**	**0.00**	**0.00**	**0.44**	**0.05**	**0.00**	**0.00**	**0.15**		**0.25**
Plagioclase	**SiO_2**	**TiO_2**	**Al_2O_3**	**Cr_2O_3**	**FeO**	**NiO**	**MnO**	**MgO**	**CaO**	**Na_2O**	**K_2O**	**Cl**	**F**	**O=F&Cl**	**TOTAL**
IEBS-2 Area 1 feldspar	62.07	0.00	22.72	0.00	0.24	0.02	0.00	0.00	4.91	7.69	0.91	0.00	0.02	-0.01	98.57
	8 oxygen atoms per formula unit (sum excludes F & Cl)														
	Si	**Ti**	**Al**	**Cr**	**Fe**	**Ni**	**Mn**	**Mg**	**Ca**	**Na**	**K**	**Cl**	**F**		**Sum**
IEBS-2 Area 1 feldspar	2.792	0.000	1.205	0.000	0.009	0.001	0.000	0.000	0.237	0.671	0.052	0.000	0.003		4.967
Clay Matrix	**SiO_2**	**TiO_2**	**Al_2O_3**	**Cr_2O_3**	**FeO**	**NiO**	**MnO**	**MgO**	**CaO**	**Na_2O**	**K_2O**	**Cl**	**F**	**O=F&Cl**	**TOTAL**
IEBS-2 Area 1 matrix	58.94	0.14	21.33	0.00	6.81	0.00	0.04	2.23	0.24	1.56	0.26	0.01	0.21	-0.09	91.56

IEBS-2 Area 3 matrix	59.02	0.12	21.19	0.00	5.06	0.01	0.01	1.75	0.32	1.04	0.29	0.01	0.23	-0.10	88.85
IEBS-2 Area 1-2 matrix	58.13	0.12	21.06	0.00	4.10	0.00	0.01	1.94	0.18	1.19	0.34	0.01	0.24	-0.10	87.10
IEBS-2 Area 4 matrix	60.06	0.11	22.16	0.00	4.60	0.00	0.01	1.82	0.29	0.93	0.26	0.01	0.19	-0.08	90.27
AVERAGE	**59.04**	**0.13**	**21.43**	**0.00**	**5.14**	**0.00**	**0.02**	**1.94**	**0.26**	**1.18**	**0.29**	**0.01**	**0.22**	**-0.09**	**89.44**
Std. Dev.	**0.79**	**0.01**	**0.50**	**0.00**	**1.17**	**0.01**	**0.02**	**0.21**	**0.06**	**0.27**	**0.04**	**0.00**	**0.02**	**0.01**	**1.92**
	12 oxygen atoms per formula unit (sum excludes F & Cl)														
	Si	**Ti**	**Al**	**Cr**	**Fe**	**Ni**	**Mn**	**Mg**	**Ca**	**Na**	**K**	**Cl**	**F**		**Sum**
IEBS-2 Area 1 matrix	4.223	0.008	1.801	0.000	0.408	0.000	0.002	0.238	0.018	0.217	0.024	0.001	0.048		6.940
IEBS-2 Area 3 matrix	4.297	0.007	1.818	0.000	0.308	0.001	0.001	0.190	0.025	0.147	0.027	0.001	0.053		6.820
IEBS-2 Area 1-2 matrix	4.297	0.007	1.835	0.000	0.253	0.000	0.001	0.214	0.014	0.171	0.032	0.001	0.056		6.823
IEBS-2 Area 4 matrix	4.289	0.006	1.865	0.000	0.275	0.000	0.001	0.194	0.022	0.129	0.024	0.001	0.043		6.804
AVERAGE	**4.28**	**0.01**	**1.83**	**0.00**	**0.31**	**0.00**	**0.00**	**0.21**	**0.02**	**0.17**	**0.03**	**0.00**	**0.05**	**#DIV/0!**	**6.85**
Std. Dev.	**0.04**	**0.00**	**0.03**	**0.00**	**0.07**	**0.00**	**0.00**	**0.02**	**0.00**	**0.04**	**0.00**	**0.00**	**0.01**	**#DIV/0!**	**0.06**
Shard (Clinoptilolite?)	**SiO_2**	**TiO_2**	**Al_2O_3**	**Cr_2O_3**	**FeO**	**NiO**	**MnO**	**MgO**	**CaO**	**Na_2O**	**K_2O**	**Cl**	**F**	**O=F&Cl**	**TOTAL**
IEBS-2 Area 1-2 shard	71.66	0.01	12.01	0.00	0.20	0.01	0.04	0.13	2.33	1.60	0.10	0.00	0.00	0.00	88.08
IEBS-2 Area 1-2 shard	71.59	0.00	11.64	0.00	0.18	0.01	0.04	0.15	1.53	2.27	0.24	0.00	0.00	0.00	87.64
IEBS-2 Area 1-2 shard	69.62	0.00	11.55	0.00	0.22	0.00	0.03	0.13	1.85	1.40	0.11	0.00	0.02	-0.01	84.92
IEBS-2 Area 1 shard	68.13	0.00	10.28	0.00	0.15	0.00	0.02	0.07	2.22	1.88	0.17	0.00	0.00	0.00	82.92
IEBS-2 Area 1-2- shard	59.92	0.00	9.27	0.00	0.24	0.00	0.01	0.12	1.20	1.91	0.17	0.11	0.01	-0.03	72.97
IEBS-2 Area 3 shard	61.68	0.00	9.37	0.00	0.23	0.00	0.02	0.15	2.49	1.67	0.07	0.00	0.09	-0.04	75.69
IEBS-2 Area 4 shard	64.31	0.00	7.16	0.00	0.15	0.00	0.02	0.15	1.69	1.90	0.13	0.00	0.00	0.00	75.52
AVERAGE	**66.70**	**0.00**	**10.18**	**0.00**	**0.20**	**0.00**	**0.03**	**0.13**	**1.90**	**1.80**	**0.14**	**0.02**	**0.02**	**-0.01**	**81.10**
Std. Dev.	**4.76**	**0.00**	**1.73**	**0.00**	**0.04**	**0.00**	**0.01**	**0.03**	**0.47**	**0.28**	**0.06**	**0.04**	**0.03**	**0.02**	**6.27**
	18 oxygen atoms per formula unit (sum excludes F & Cl)														
	Si	**Ti**	**Al**	**Cr**	**Fe**	**Ni**	**Mn**	**Mg**	**Ca**	**Na**	**K**	**Cl**	**F**		**Sum**
IEBS-2 Area 1-2 shard	7.629	0.001	1.507	0.000	0.018	0.000	0.003	0.021	0.266	0.329	0.013	0.000	0.000		9.788
IEBS-2 Area 1-2 shard	7.663	0.000	1.469	0.000	0.016	0.000	0.003	0.023	0.175	0.471	0.032	0.001	0.000		9.854
IEBS-2 Area 1-2 shard	7.666	0.000	1.498	0.000	0.021	0.000	0.003	0.022	0.218	0.299	0.016	0.001	0.007		9.742
IEBS-2 Area 1 shard	7.713	0.000	1.371	0.000	0.015	0.000	0.002	0.012	0.269	0.412	0.025	0.001	0.000		9.820
IEBS-2 Area 1-2- shard	7.711	0.000	1.406	0.000	0.026	0.000	0.001	0.023	0.166	0.475	0.029	0.025	0.004		9.838
IEBS-2 Area 3 shard	7.673	0.000	1.373	0.000	0.023	0.000	0.003	0.028	0.332	0.402	0.012	0.000	0.035		9.847
IEBS-2 Area 4 shard	7.962	0.000	1.045	0.000	0.015	0.000	0.003	0.027	0.224	0.457	0.020	0.000	0.002		9.754
AVERAGE	**7.72**	**0.00**	**1.38**	**0.00**	**0.02**	**0.00**	**0.00**	**0.02**	**0.24**	**0.41**	**0.02**	**0.00**	**0.01**		**9.81**

Std. Dev.	**0.11**	**0.00**	**0.16**	**0.00**	**0.00**	**0.00**	**0.00**	**0.01**	**0.06**	**0.07**	**0.01**	**0.01**	**0.01**		**0.05**
Stilpnomelane	**SiO_2**	**TiO_2**	**Al_2O_3**	**Cr_2O_3**	**FeO**	**NiO**	**MnO**	**MgO**	**CaO**	**Na_2O**	**K_2O**	**Cl**	**F**	**O=F&Cl**	**TOTAL**
IEBS-2 Area 2 Stilp?	34.60	0.00	11.14	0.00	31.40	0.01	0.09	1.27	5.85	2.51	0.03	0.15	0.06	-0.06	87.05
IEBS-2 Area 3 stilp?	41.95	0.05	16.08	0.01	29.64	0.02	0.14	1.68	0.76	2.98	0.14	0.07	0.00	-0.02	93.53
IEBS-2 Area 3 stilp?	36.58	0.02	15.09	0.01	27.74	0.02	0.13	1.73	0.59	2.41	0.16	0.09	0.01	-0.03	84.56
IEBS-2 Area 3 stilp?	38.07	0.02	15.82	0.00	30.21	0.01	0.15	1.54	0.78	3.57	0.15	0.06	0.11	-0.06	90.38
AVERAGE	**37.80**	**0.02**	**14.53**	**0.01**	**29.75**	**0.02**	**0.13**	**1.55**	**1.99**	**2.87**	**0.12**	**0.09**	**0.04**	**-0.04**	**88.88**
Std. Dev.	**3.11**	**0.02**	**2.30**	**0.01**	**1.53**	**0.01**	**0.03**	**0.21**	**2.57**	**0.53**	**0.06**	**0.04**	**0.05**	**0.02**	**3.91**
	18 oxygen atoms per formula unit (sum excludes F & Cl)														
	Si	**Ti**	**Al**	**Cr**	**Fe**	**Ni**	**Mn**	**Mg**	**Ca**	**Na**	**K**	**Cl**	**F**		**Sum**
IEBS-2 Area 2 Stilp?	7.671	0.000	2.911	0.000	5.822	0.002	0.017	0.420	1.390	1.079	0.008	0.056	0.042		19.38
IEBS-2 Area 3 stilp?	8.171	0.007	3.691	0.002	4.828	0.003	0.023	0.488	0.159	1.125	0.035	0.023	0.000		18.56
IEBS-2 Area 3 stilp?	7.938	0.003	3.859	0.002	5.034	0.003	0.024	0.560	0.137	1.014	0.044	0.033	0.007		18.65
IEBS-2 Area 3 stilp?	7.799	0.003	3.820	0.000	5.176	0.002	0.026	0.470	0.171	1.418	0.039	0.021	0.071		18.95
AVERAGE	**7.89**	**0.00**	**3.57**	**0.00**	**5.21**	**0.00**	**0.02**	**0.48**	**0.46**	**1.16**	**0.03**	**0.03**	**0.03**		**18.88**
Std. Dev.	**0.21**	**0.00**	**0.45**	**0.00**	**0.43**	**0.00**	**0.00**	**0.06**	**0.62**	**0.18**	**0.02**	**0.02**	**0.03**		**0.37**

IEBS-2 Steel															
Fe-saponite	**SiO_2**	**TiO_2**	**Al_2O_3**	**Cr_2O_3**	**FeO**	**NiO**	**MnO**	**MgO**	**CaO**	**Na_2O**	**K_2O**	**Cl**	**F**	**O=F&Cl**	**TOTAL**
IEBS-2 Steel Area 1 Fe sap	41.79	0.03	16.85	0.17	29.86	0.24	0.29	1.52	0.89	3.86	0.06	0.01	0.01	-0.01	95.58
IEBS-2 Steel Area 1 Fe sap	43.70	0.06	16.35	0.15	27.16	0.23	0.25	1.57	0.92	3.24	0.07	0.02	0.00	-0.01	93.73
IEBS-2 Steel Area 1 Fe sap	41.41	0.04	17.17	0.18	29.27	0.23	0.24	1.50	0.85	3.60	0.08	0.02	0.00	0.00	94.60
IEBS-2 Steel Area 1 Fe sap	35.41	0.02	15.74	0.33	34.11	0.29	0.33	1.20	0.45	2.58	0.08	0.01	0.03	-0.02	90.57
IEBS-2 Steel Area 4 Fe sap	41.10	0.03	16.11	0.23	27.33	0.40	0.22	1.58	0.14	4.19	0.17	0.08	0.08	-0.05	91.59
IEBS-2 Steel Area 4 Fe sap	33.77	0.03	15.05	0.22	25.55	0.25	0.26	1.46	0.08	5.65	0.10	0.09	0.06	-0.04	82.52
AVERAGE	**39.53**	**0.04**	**16.21**	**0.21**	**28.88**	**0.27**	**0.27**	**1.47**	**0.56**	**3.86**	**0.09**	**0.04**	**0.03**	**-0.02**	**91.43**
Std. Dev.	**3.97**	**0.01**	**0.77**	**0.07**	**3.00**	**0.07**	**0.04**	**0.14**	**0.39**	**1.04**	**0.04**	**0.04**	**0.03**	**0.02**	**4.75**
	12 oxygen atoms per formula unit (sum excludes F & Cl)														
	Si	**Ti**	**Al**	**Cr**	**Fe**	**Ni**	**Mn**	**Mg**	**Ca**	**Na**	**K**	**Cl**	**F**		**Sum**
IEBS-2 Steel Area 1 Fe sap	3.434	0.002	1.632	0.011	2.052	0.016	0.020	0.186	0.079	0.614	0.006	0.002	0.002		8.053
IEBS-2 Steel Area 1 Fe sap	3.587	0.004	1.581	0.010	1.864	0.015	0.018	0.192	0.081	0.516	0.008	0.002	0.001		7.876
IEBS-2 Steel Area 1 Fe sap	3.426	0.003	1.675	0.012	2.025	0.015	0.017	0.186	0.075	0.578	0.008	0.002	0.000		8.021
IEBS-2 Steel Area 1 Fe sap	3.196	0.001	1.674	0.024	2.575	0.021	0.025	0.162	0.044	0.452	0.010	0.001	0.009		8.185
IEBS-2 Steel Area 4 Fe sap	3.497	0.002	1.615	0.015	1.945	0.027	0.016	0.200	0.013	0.691	0.019	0.012	0.020		8.041
IEBS-2 Steel Area 4 Fe sap	3.267	0.002	1.716	0.017	2.067	0.019	0.021	0.210	0.008	1.060	0.012	0.015	0.018		8.401
AVERAGE	**3.40**	**0.00**	**1.65**	**0.01**	**2.09**	**0.02**	**0.02**	**0.19**	**0.05**	**0.65**	**0.01**	**0.01**	**0.01**		**8.10**
Std. Dev.	**0.15**	**0.00**	**0.05**	**0.01**	**0.25**	**0.00**	**0.00**	**0.02**	**0.03**	**0.22**	**0.00**	**0.01**	**0.01**		**0.18**
Chlorite?	**SiO_2**	**TiO_2**	**Al_2O_3**	**Cr_2O_3**	**FeO**	**NiO**	**MnO**	**MgO**	**CaO**	**Na_2O**	**K_2O**	**Cl**	**F**	**O=F&Cl**	**TOTAL**
IEBS-2 Steel Area 3 chl?	46.02	0.10	21.84	0.12	5.98	0.10	0.06	1.57	0.19	2.29	0.35	0.01	0.23	-0.10	78.63
IEBS-2 Steel Area 3 chl?	62.39	0.12	21.12	0.07	6.69	0.11	0.01	1.97	0.22	1.42	0.43	0.01	0.17	-0.08	94.58
AVERAGE	**54.20**	**0.11**	**21.48**	**0.09**	**6.33**	**0.11**	**0.04**	**1.77**	**0.21**	**1.85**	**0.39**	**0.01**	**0.20**	**-0.09**	**86.60**
Std. Dev.	**11.58**	**0.01**	**0.51**	**0.03**	**0.51**	**0.01**	**0.04**	**0.28**	**0.03**	**0.62**	**0.06**	**0.00**	**0.04**	**0.02**	**11.27**
	11 oxygen atoms per formula unit (sum excludes F & Cl)														
	Si	**Ti**	**Al**	**Cr**	**Fe**	**Ni**	**Mn**	**Mg**	**Ca**	**Na**	**K**	**Cl**	**F**		**Sum**
IEBS-2 Steel Area 3 chl?	3.570	0.006	1.997	0.007	0.388	0.006	0.004	0.182	0.016	0.344	0.035	0.001	0.056		6.56
IEBS-2 Steel Area 3 chl?	3.957	0.006	1.579	0.004	0.355	0.006	0.001	0.186	0.015	0.175	0.035	0.001	0.034		6.32
AVERAGE	**3.76**	**0.01**	**1.79**	**0.01**	**0.37**	**0.01**	**0.00**	**0.18**	**0.02**	**0.26**	**0.03**	**0.00**	**0.05**		**6.44**
Std. Dev.	**0.27**	**0.00**	**0.30**	**0.00**	**0.02**	**0.00**	**0.00**	**0.00**	**0.00**	**0.12**	**0.00**	**0.00**	**0.02**		**0.17**

Appendix D

SEM Images

IEBS-1

SEM Images

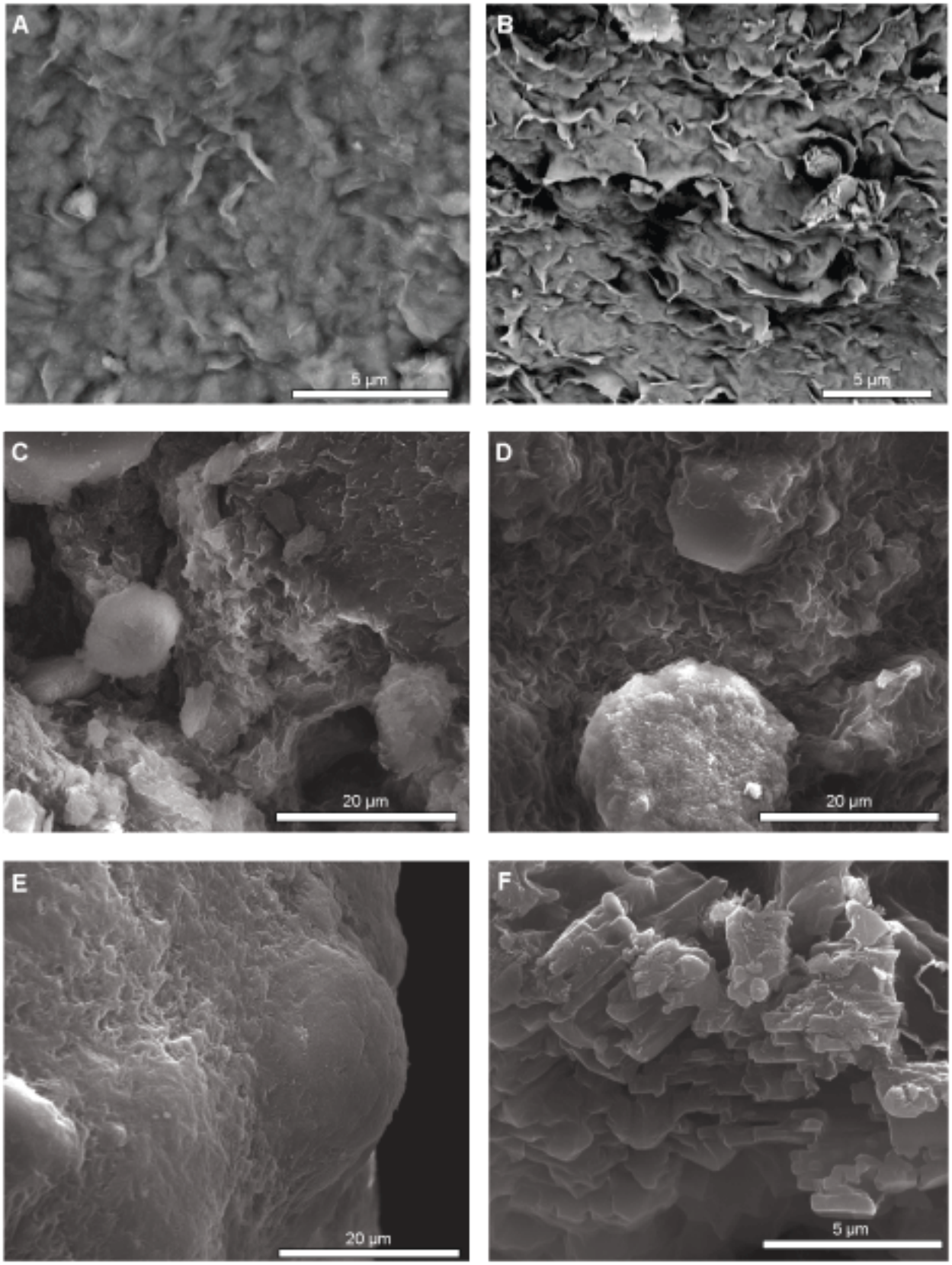

Figure D-1. IEBS-1 secondary electron images. **[A]** Montmorillonite transitioning to smectite**. [C, D, E]** SEM images of C(A)SH crystals in the smectite matrix**. [F]** Albite crystals, note that these albite crystals are corroding.

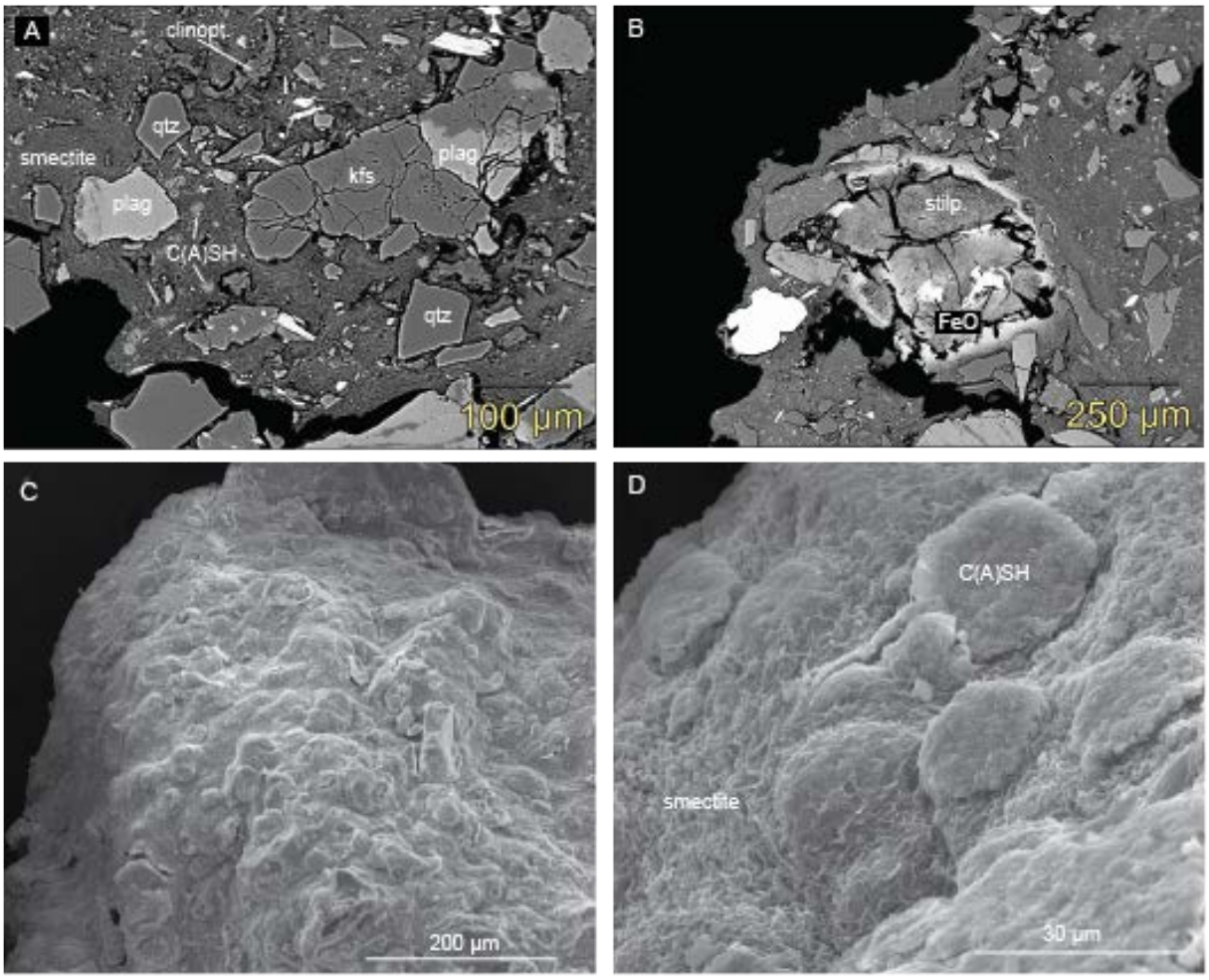

Figure D-2. IEBS-1. **[A]** BSE image of an IEBS-1 thin section showing feldspar, quartz, C(A)SH minerals, and glass shards in a smectite matrix. **[B]** Stilpnomelane growth around a grain of FeO (buffer material) in a smectite matrix. **[C]** Secondary electron image of C(A)SH mineral growth in smectite. **[D]** Zoomed in view of area **[C]**. Abbreviations: C(A)SH, calcium (aluminum) silicate hydrate; clinopt, clinoptilolite; kfs, K-feldspar; plag, plagioclase; qtz, quartz.

IEBS-2

SEM Images

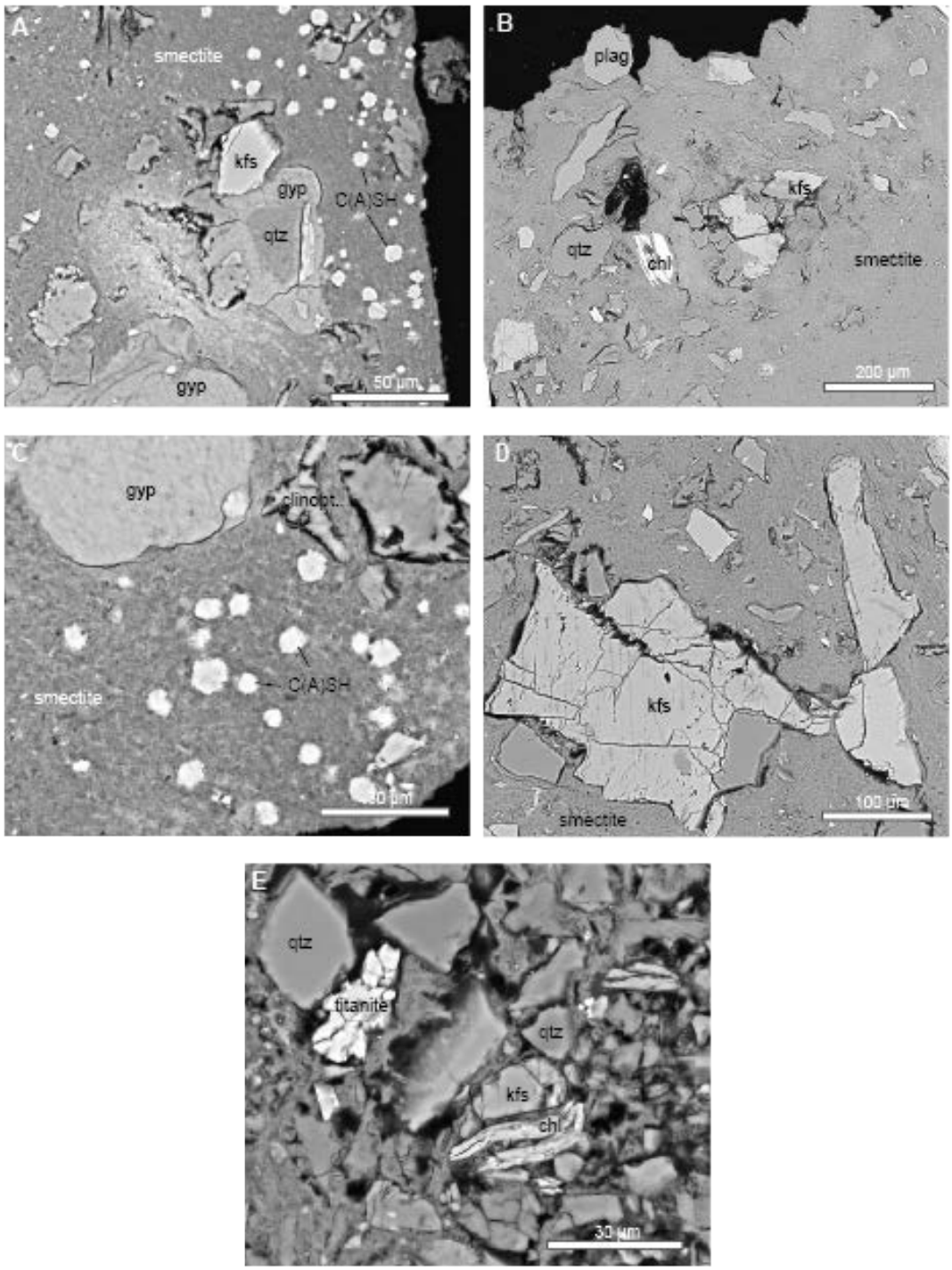

Figure D-3. IEBS-2. Backscattered electron images from IEBS-2 (thin section). Labelled minerals were identified with EDS. **[A–D]** Feldspar, quartz, and gypsum in the fine-grained clay matrix **[A, C]** White spherical minerals are C(A)SH minerals. **[E]** Grimsel Granodiorite fragment composed of feldspars, quartz, chlorite, and accessory minerals (e.g., titanite). Abbreviations: C(A)SH, calcium (aluminum) silicate hydrate; chl, chlorite; gyp, gypsum; kfs, K-feldspar; plag, plagioclase; qtz, quartz.

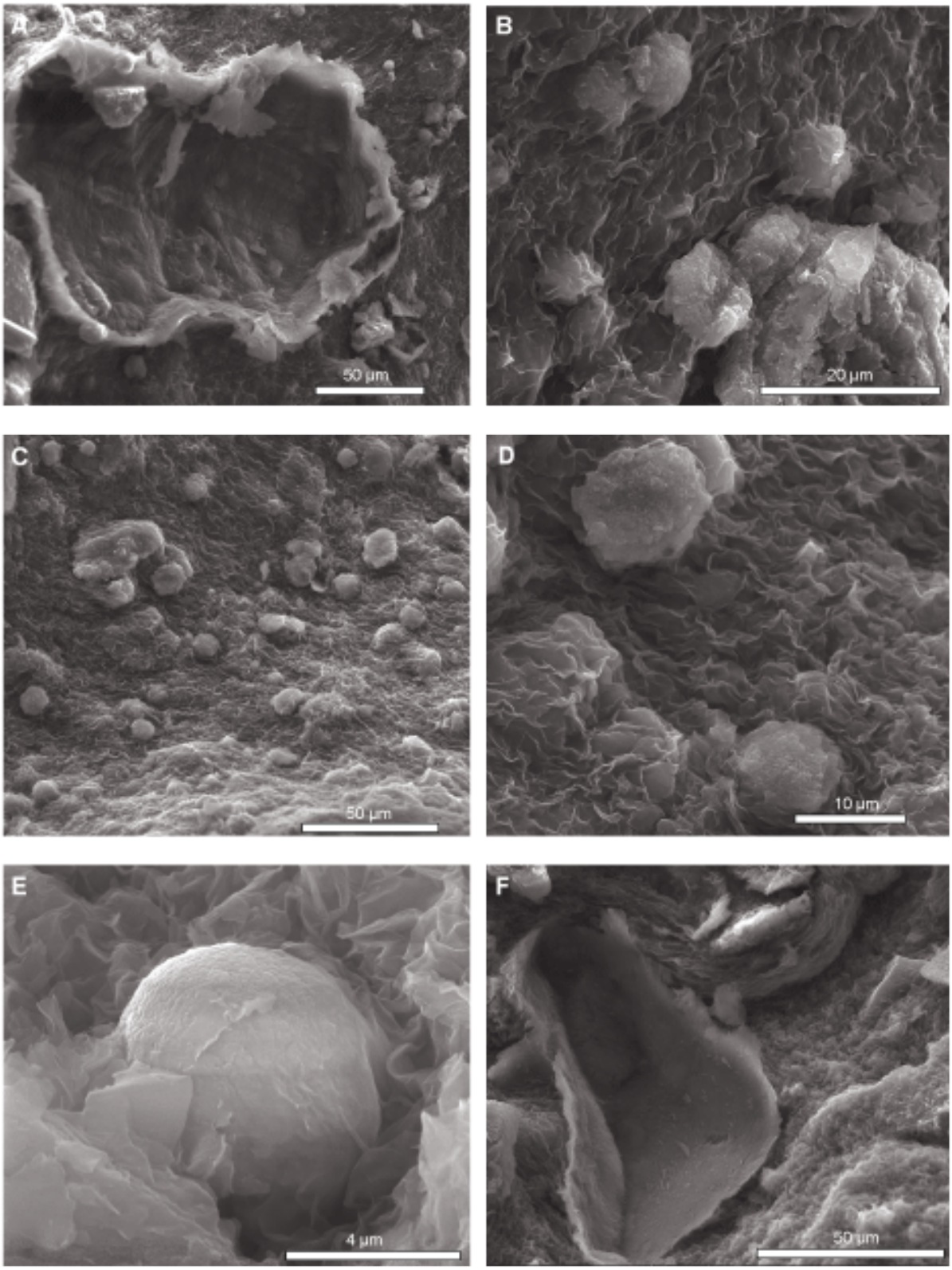

Figure D-4. IEBS-2 secondary electron images. **[A, F]** Chlorite fragment from original host granodiorite. **[B, C, D]** Juvenile-to-mature C(A)SH crystals embedded in smectite matrix. **[E]** C(A)SH crystal embedded in smectite.

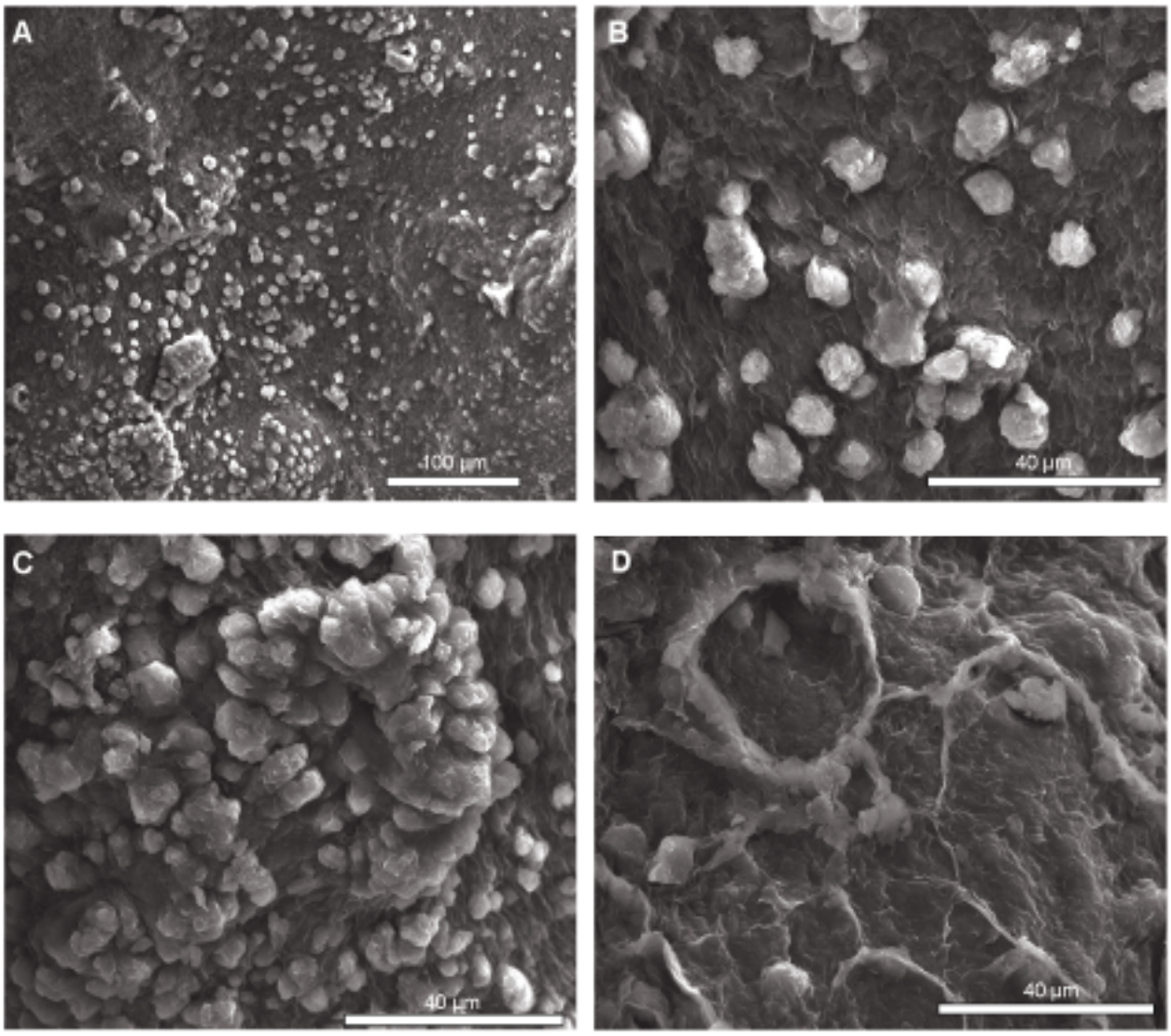

Figure D-5. IEBS-2. **[A, B, C]** Secondary electron images of gypsum crystals embedded in smectite matrix and **[D]** mixed phases of C(A)SH crystals and secondary feldspars.

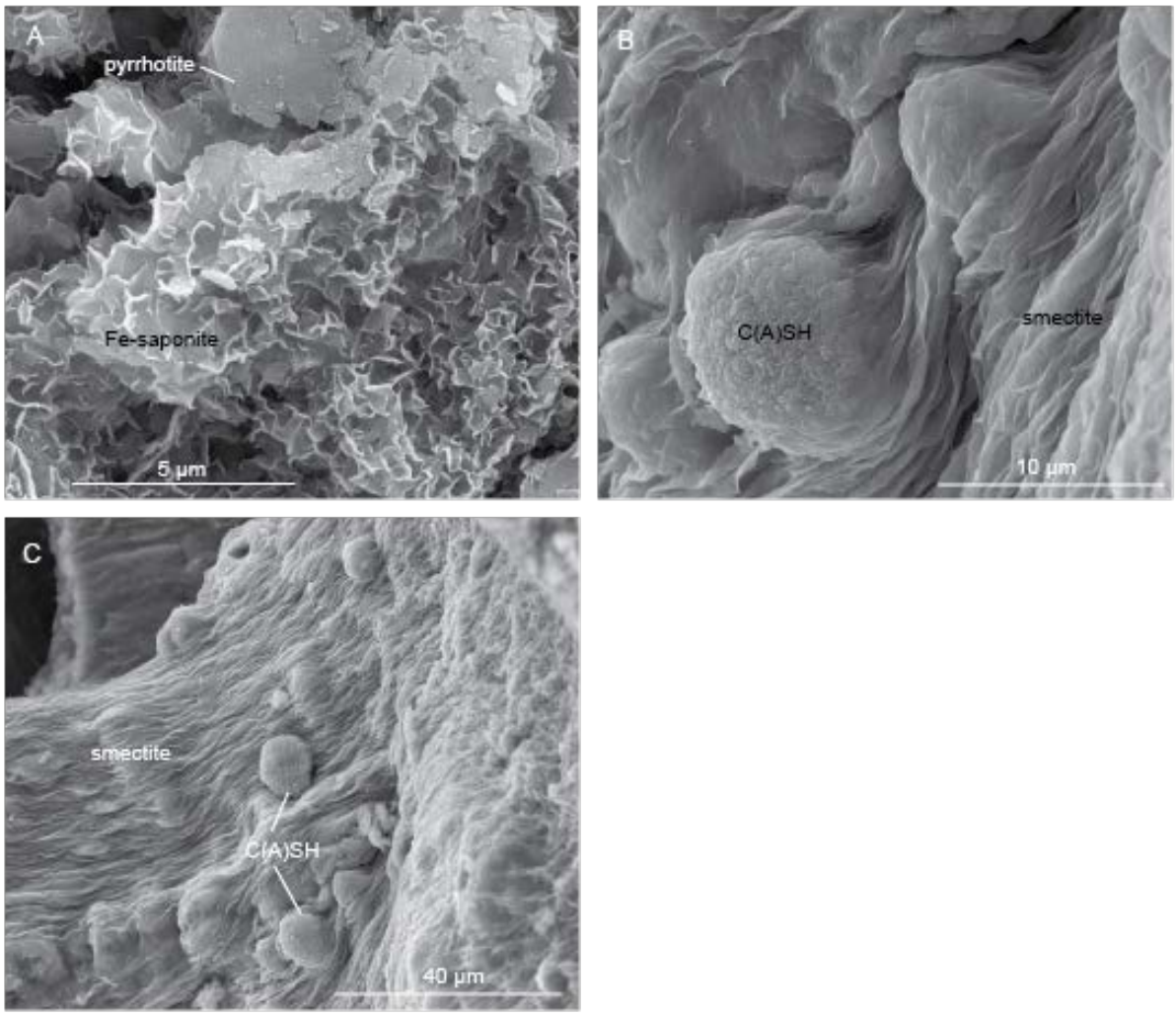

Figure D-6. Secondary electron images of IEBS-2 reaction products. **[A]** Fe-saponite and pyrrhotite that likely formed at the interface of the 316 SS and the Wyoming bentonite. **[B, C]** C(A)SH minerals embedded in smectite.

Appendix E

FCT Document Cover Sheet

Revision 3
10/01/2016

APPENDIX E

FCT DOCUMENT COVER SHEET [1]

Name/Title of Deliverable/Milestone/Revision No.	Engineered Barrier System R&D and International Collaborations – LANL
Work Package Title and Number	Engineered Barrier System R&D - LANL/ Engineered Barrier System International Collaborations - LANL
Work Package WBS Number	SF-18LA01030801/ SF-18LA01030805
Responsible Work Package Manager	Florie Caporuscio (Name/Signature)
Date Submitted	August 10. 2018

Quality Rigor Level for Deliverable/Milestone[2]	☐ QRL-1 Nuclear Data	☐ QRL-2	☐ QRL-3	■ QRL 4 Lab-specific

This deliverable was prepared in accordance with Los Alamos National Laboratory
(Participant/National Laboratory Name)

QA program which meets the requirements of
☐ DOE Order 414.1 ☐ NQA-1 ☐ Other

This Deliverable was subjected to:

☐ Technical Review

Technical Review (TR)

Review Documentation Provided

☐ Signed TR Report or,
☐ Signed TR Concurrence Sheet or,
☐ Signature of TR Reviewer(s) below

Name and Signature of Reviewers

☐ Peer Review

Peer Review (PR)

Review Documentation Provided

☐ Signed PR Report or,
☐ Signed PR Concurrence Sheet or,
■ Signature of PR Reviewer(s) below

Name and Signature of Reviewers

Frank Perry

NOTE 1: *Appendix E should be filled out and submitted with each deliverable. Or, if the PICS:NE system permits, completely enter all applicable information in the PICS:NE Deliverable Form. The requirement is to ensure that all applicable information is entered either in the PICS:NE system or by using the FCT Document Cover Sheet.*

- *In some cases there may be a milestone where an item is being fabricated, maintenance is being performed on a facility, or a document is being issued through a formal document control process where it specifically calls out a formal review of the document. In these cases, documentation (e.g., inspection report, maintenance request, work planning package documentation or the documented review of the issued document through the document control process) of the completion of the activity, along with the Document Cover Sheet, is sufficient to demonstrate achieving the milestone.*

NOTE 2: *If QRL 1, 2, or 3 is not assigned, then the QRL 4 box must be checked, and the work is understood to be performed using laboratory specific QA requirements. This includes any deliverable developed in conformance with the respective National Laboratory / Participant, DOE or NNSA-approved QA Program.*